Swart, P.K., Eberli, G.P., Malone, M.J., and Sarg, J.F. (Eds.), 2000
Proceedings of the Ocean Drilling Program, Scientific Results, Vol. 166

6. MINERALOGY AND SEDIMENTOLOGY OF THE PLEISTOCENE TO HOLOCENE ON THE LEEWARD MARGIN OF GREAT BAHAMA BANK[1]

Rebecca H. Rendle,[2] John J.G. Reijmer,[2] Dick Kroon,[3] Gideon M. Henderson[4]

ABSTRACT

The mineralogy of periplatform carbonates is well documented in the literature. However, little is written about the grain-size properties for carbonate rocks. This fundamental property forms a controlling factor for other derived physical properties such as bulk density, porosity, and permeability. Thus, grain-size distribution and sorting might also steer fluid flow through the sediments, and combined with the mineralogy, might affect the development of the initial diagenetic pattern, which is significant in the interpretation of ancient depositional environments and transport conditions.

This study, therefore, documents grain-size variations in conjunction with carbonate mineralogy for periplatform oozes of Sites 1003 (mid-slope) and 1006 (basin) on the leeward side of the Great Bahama Bank. The results reveal some distinct differences between glacial periods (glacials) and interglacial periods (interglacials) through both time and space.

The $\delta^{18}O$ and aragonite stratigraphy shows an almost complete sedimentary record for Site 1006, which is supported in the upper section by the U/Th dates assigned to interglacial Stages 1, 5, 9, and 11. However, Site 1003 stratigraphy indicates that large hiatuses exist within the sedimentary record and that there is evidence for diagenetic overprinting. This interpretation is further supported by the U/Th dates provided.

Glacials are represented by sediment dominated by high-Mg calcite (HMC) and low-Mg calcite (LMC). The HMC probably originates from erosion of magnesium-calcite micrite cements formed in the upper slope deposits or HMC cements formed during early diagenesis. Detrital dolomite is also present at the distal site (Site 1006). Quartz also occurs preferentially during these periods. Although the grain-size distribution shows dominance by silts and clays (i.e., fine fraction [<63 µm]) the percentage of the coarse fraction (>63 µm) increases markedly during glacials. The latter fraction shows an increased dominance by the coarse (500–1000 µm) to very coarse (>1000 µm) sand-size fractions.

Interglacials, in contrast, are dominated by aragonite, mainly in the form of fine-grained, bank-top -derived aragonite needles. This is supported by the grain-size distribution, which again shows dominance by silts and clays (<63 µm). Dolomite is present at Site 1003, originating from early diagenesis. The coarse fraction (>63 µm) is dominated by the very fine (63–125 µm) to medium (250–500 µm) sand-sized particles.

Therefore, the fine-grained interglacial deposits will have a low diagenetic potential because of restricted fluid flow and low permeability, whereas the glacials will show the reverse pattern where the coarse-grained sediment facilitates early diagenesis. The diagenetic potential of the sediment on the leeward side of the Great Bahama Bank, therefore, varies through both time (between glacial and interglacials) and space (decreasing in potential with increasing distance from the platform). The composition of the coarse grains (63 µm) exported from the platform during glacial and interglacials forms the key link in understanding the mineralogy and grain-size data, and thus is the main topic of work in progress.

INTRODUCTION

Carbonate slopes receive, lose, and store sediments through the interplay of deposition, erosion, cementation, and dissolution. The development of accretionary or erosive slopes mainly depends on the slope angle (Schlager and Camber, 1986). Increase in slope angle will shift the activity of gravity flows from depositional to erosional, and thus control the type of sedimentary deposits seen in this environment. In addition, the type of sediment stored on the slope will control the slope declivity.

Kenter (1990) clearly showed that carbonate muds are not able to maintain a slope that exceeds 5°, whereas coarse-grained deposits can build slopes with an angle of up to 32°. The grain size of the sediments produced on the platform will, therefore, play an important role in determining the type of slope that might develop.

The present-day morphology of the Bahamas shows shallow-water platforms that are separated from deep-water areas by relatively steep slopes. On the leeward side, the slope profile displays a 4-km-wide gently sloping interval between the platform interior and the slope break at 55–65 m water depth (Wilber et al., 1990). Seaward of the slope break, gradients increase to a water depth of 140–180 m, forming an almost vertical wall. At the base of this wall, a 30-m-wide trough is present. This is followed by a 100- to 200-m-wide depositional ridge that shoals for about 40 m. Westward of this elevation, the slope continues with angles between 15° and 20° (Wilber et al., 1990). Slopes in the Tongue of the Ocean (windward margin of the Great Bahama Bank) have a more regular topography (Grammer et al., 1991; Grammer and Ginsburg, 1992) whereby the profile shows a platform edge with angles ranging between 20° and 30° down to 60 m water depth, and a 60–120 m near-vertical wall (65°–90°), followed by a steeply inclined 32°–38° slope that gradually decreases to angles of 25°–28° down into the basin (Grammer et al., 1991; Grammer and Ginsburg, 1992).

Grammer et al. (1991) also showed that slope development on the windward margin differs from that on the leeward margin in the Tongue of the Ocean. The most striking feature is the variable thickness of the unconsolidated fine-grained sediments onlapping the cemented slope. The leeward slope displays some areas of larger sediment wedges onlapping the cemented slopes when compared with its windward counterparts. The extensive sediment wedge present on the western leeward side of the Great Bahama Bank fits into this model. High-resolution seismic profiles show large-scale export of bank-top sediment and rapid progradation of the slope during the Holocene along the leeward slope of the western Great Bahama Bank (Wilber

[1]Swart, P.K., Eberli, G.P., Malone, M.J., and Sarg, J.F. (Eds.), 2000. *Proc. ODP, Sci. Results,* 166: College Station TX (Ocean Drilling Program).

[2]GEOMAR Forschungszentrum für marine Geowissenschaften, Wischhofstr. 1-3, D-24148 Kiel, Federal Republic of Germany. Correspondence author: rrendle@geomar.de

[3]The University of Edinburgh, Grant Institute, West Mains Road, Edinburgh EH9 3JW, Scotland.

[4]Oxford University, the Department of Earth Sciences, Park Road, Oxford OX1 3PR, England.

et al., 1990). Variations in the relative position in sea level during the last 18 k.y. (isotope Stages 1 and 2) played an important role in the development of the aforementioned slope profiles (Grammer and Ginsburg, 1992).

Purdy (1963) and Enos (1974) have provided a detailed description of the sediment facies that are found on the present-day Great Bahama Bank. Neumann and Land (1975) made some gross calculations on the production potential of the shallow-water realm and found that large quantities of fine-grained carbonate mud are exported from the platform into the basin. Studies by Boardman and Neumann (1984, 1986), Boardman et al. (1986), Milliman et al. (1993), and Robbins et al. (1997), among others, have demonstrated the production of the fine-grained sediments on the platform top and the subsequent export to the basinal realm. Sediment-charged hyperpycnal (high density) waters are able to transport the entrapped sediment over large distances (Wilson and Roberts, 1995); therefore, this process, called "density cascading," might enhance the export of fine-grained, shallow-water material from the platform top. Hyperpycnal waters are generated in shoal waters through thermohyaline processes. Climatic changes steer the possibility that rapid water-mass modifications occur, and thus create variations in the number of density cascading events that might well evolve through time (Wilson and Roberts, 1995).

The mineralogy of the sediments on the platform top is mainly dominated by aragonite (e.g., Pilkey and Rucker, 1966; Milliman, 1974; Droxler, 1984). The variations in sediment export toward the basin will, therefore, display themselves as variations in the input of aragonite. Studies by Droxler et al. (1983), Boardman and Neumann (1984), Droxler et al. (1988), and Reijmer et al. (1988) clearly demonstrated this principle in cores taken in the Tongue of the Ocean and Exuma Sound. In addition, these periplatform sediments show a good agreement between the oxygen isotopes and the carbonate mineralogy (e.g., Droxler et al., 1983). This link might then provide us with a correlation to the observed climatic changes for these surroundings as described by Kroon et al. (Chap. 2, this volume).

The succession researched in this paper is deposited in a time slice in which the Great Bahama Bank shows an overall progradation pattern clearly visible in the regional seismic line known as "the Western Line" (Eberli and Ginsburg, 1987, 1989). Shallowing-upward trends found in the sediments recovered in the boreholes CLINO and UNDA (Eberli, Swart, McNeill, et al., 1997) confirm this general trend. It is, therefore, plausible that Sites 1003 and 1006 described in this paper were influenced more and more by the advancing platform. In connection with increased production on the platform top, this would lead to increased off-bank transport and deposition, which would invariably play an important role in the sediment development of the slope.

This paper will concentrate on variations in the mineralogy and grain-size distribution at two sites on the leeward side of the Great Bahama Bank. Site 1003, situated proximally to the platform, is positioned above thick lower slope sections and is, therefore, an ideal place to evaluate lowstand vs. highstand input signals. The distal site, Hole 1006A, then provides a more pelagic reference signal for this lowstand vs. highstand variations. As already demonstrated by Westphal (1997) and Westphal et al. (1999), the grain size in combination with the mineralogy plays an important role in the diagenesis pattern that develops within the sediments. The initial permeability seems to influence the nature of the diagenesis (Westphal, 1997). Slope sediments from the Great Bahama Bank (the CLINO core; see Eberli, Swart, McNeill, et al., 1997) showed that coarse-grained deposits with their initial high permeabilities were subjected to intense diagenetic alteration. Unlike the coarse-grained lowstand sediments, the fine-grained highstand deposits were protected against large initial fluid-flow alterations because of their low permeability (Westphal, 1997). The way in which the mineralogy and grain-size distribution is developed through time and space along the platform slope will be of great interest for later diagenetic studies.

As will be shown, both mineralogy and grain-size distributions are good proxies to determine environmental variations through time. The analysis of the different sedimentation patterns developed during glacial and interglacial periods (interglacials) might help us to understand in detail the response of the shallow-water production area of the Great Bahama Bank to changes in climate.

As mentioned above, variations in the mineralogy and the grain size will modify the diagenetic potential of the sediments. It is important to understand what types of patterns develop on a vertical (time) and a lateral (spacial) scale. Understanding these patterns in the present-day environment might then help us when analyzing ancient platform-to-basin transects.

REGIONAL SETTING

Sites 1003 and 1006 were drilled on the prograding western margin of the Great Bahama Bank during Ocean Drilling Program (ODP) Leg 166. Both sites lie along a platform-to-basin transect that connects the shallow bank with the deeper water areas. This transect was positioned on the "Western Geophysical seismic line" studied previously by Eberli and Ginsburg (1987, 1989) (Fig. 1). The more proximal site, Site 1003, represents the middle-slope sediments and is situated ~4 km from the platform edge at a water depth of 481 meters below sea level (mbsl). Site 1006, in contrast, is the most distal site along the transect located basinward in the northern portion of the Santaren Channel ~30 km from the platform edge at a water depth of 658 mbsl. This site was designed to (1) provide an independent indicator of sea level because of its greater pelagic component, and (2) through sequence stratigraphy, aid in the dating of the proximal sites where the chronostratigraphy is occasionally unclear. This lack of clarity could be the result of missing sequences because of erosion and/or poor recovery, and diagenesis and/or dilution by neritic sediments (Eberli, Swart, Malone, et al., 1997).

The sediments in the interval studied (0–77.5 meters below seafloor [mbsf]) at Site 1003 are Pleistocene to Holocene in age and consist primarily of unlithified to partially lithified mudstones to floatstones and minor nannofossil oozes, which contain approximately equal amounts of platform-derived mud and calcareous sand mixed with pelagic carbonate components (i.e., periplatform ooze; Schlager and James, 1978). Peloids and aragonite needles are also major components through this section. This sediment interval lies within lithostratigraphic Unit I (0–162.1 mbsf; Eberli, Swart, Malone, et al., 1997). The upper interval (0–59.9 mbsf) is thought to show a change from pelagic-dominated input in the lower section of the interval to a strong input of coarse particles in the middle to upper part that are derived from the shallow carbonate producing area (Eberli, Swart, Malone, et al., 1997). The lower interval (59.9–162.1 mbsf), in contrast, consists of an alternation of coarser and finer grained intervals that are relatively rich in platform-derived components. A downcore disappearance of peloids was also observed.

The sediments in the interval studied at Site 1006 (0–65 mbsf) are Pliocene to Holocene in age and consist of largely unlithified, bioturbated nannofossil ooze (with sand- and silt-sized foraminifers) with a small component of aragonite needles in the upper section. This lies within lithostratigraphic Unit I (0–125.95 mbsf; Eberli, Swart, Malone, et al., 1997). The interruption of this unit by a possible hardground (a chalky layer) and a series of silty clay layers allows division of Unit I into two subunits. The upper interval (0–7.28 mbsf) is a nannofossil ooze with small amounts of aragonite needles, where particle abundance and grain size increases downcore to the base of this subunit. It is thought to reflect a mix of pelagic and bank-derived carbonates (Eberli, Swart, Malone, et al., 1997). The lower interval (7.28–125.95 mbsf) is a nannofossil ooze interbedded with clays reflecting erosion from a continental source, probably Cuba and/or Hispaniola (Eberli, Swart, Malone, et al., 1997).

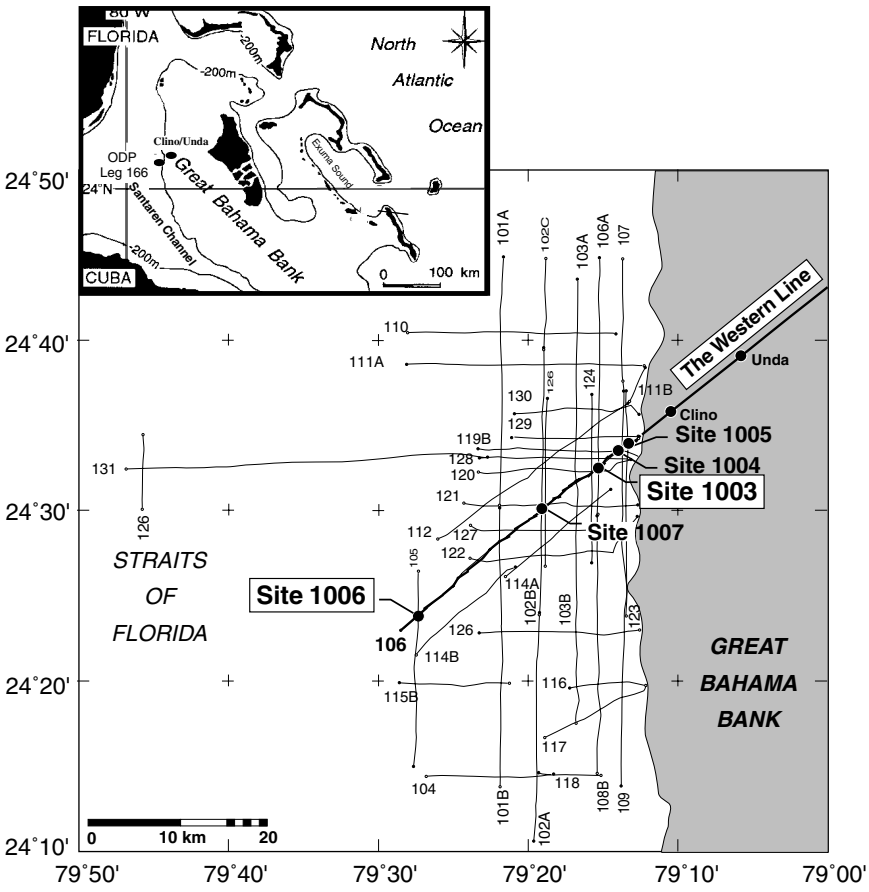

Figure 1. The top left map shows the position of ODP Leg 166 (Sites 1003–1007) and the CLINO and UNDA sites, which are situated on the leeward side of the Great Bahama Bank (taken from Kindler and Hearty, 1996). The main map (after Eberli, Swart, Malone, et al., 1997) gives the position of the individual sites, which run in an east-northeast–west-southwest direction along seismic Line 106, "The Western Line." Sites 1003 and 1006 are highlighted to indicate their positions along the transect.

METHODS

All samples used for analysis consist of 15 cm^3 of sediment taken at a general sampling frequency of 20 cm within each core. However, additional samples were taken in between to increase the sampling frequency at significant points (e.g., transitions between glacial periods [glacials] and interglacials). A total of 454 samples have been analyzed from Hole 1003A (Sections 166-1003A-1H-01 through 9H-CC) and a total of 293 samples were taken from Hole 1006A (Sections 166-1006A-1H-01 through 7H-7). A flow diagram to in Figure 2 shows the laboratory procedures.

Oxygen Isotope Analysis

The samples (5 cm^3) were oven dried at 45°C, weighed, and then washed through a 63-µm stainless steel sieve. The coarse fraction was then further divided into subfractions (for details, see "Sediment Flux Analysis"). The 250- to 500-µm fraction was used to pick tests of the planktonic foraminiferal species *Globigerinoides ruber*. Care was taken to select only complete and undamaged tests to reduce the risk of picking the incorrect species. The tests were then soaked in methyl alcohol for several minutes and cleaned in an ultrasonic bath to remove adherent contaminants. Following ultrasonic cleaning, excess methyl alcohol was drawn off with tissue paper, and any residual alcohol was allowed to evaporate. The foraminiferal sample weights were typically <0.1 mg and composed of 5–8 planktonic specimens.

After cleaning, the foraminiferal tests were reacted in orthophosphoric acid (specific gravity = 1.9) at 90°C, and the resulting CO_2 gas was analyzed using a Precision Isotope Ratio Mass Spectrometer (PRISM) located at the Geology and Geophysics Department of the University of Edinburgh. The samples were analyzed using an internal laboratory standard (marble reference SM1), and the values obtained converted to a PeeDee Belemnite (PDB) standard. Precision for the oxygen isotope analysis was 0.085° (standard deviation for 100 analyses of an "in-house" standard carbonate [SM1] conducted over several months) using SM1 sample weights of 0.05–0.1 mg.

X-ray Diffraction Analysis

The analysis was carried out on ~0.5 g of fine-fraction (<63 µm) sediment, and follows that described in various texts including Milliman (1974). Each sample was oven dried at 60°C before being ground for exactly 4 min in an agate mortar (with analytical grade acetone). This provides a more homogenized sediment, and thus reduces errors that might seriously affect the quality of the results. The grinding time has been documented as that required to provide an optimal peak intensity for X-ray diffraction (XRD) analysis (Milliman, 1974).The individual samples were then drawn up in a pipette, dispersed on a glass slide (2-cm diameter), smeared out to produce a sediment slurry of standard thickness and diameter, and dried at room temperature before being subjected to X-rays.

The samples were analyzed at the Geology and Geophysics Department of the University of Edinburgh using a Philips PW 1011/1050 automatic power diffractometer (PW 1808 sample charger) at 40 kV and 50 mA, through a scan from 25° to 45° 2-θ, at a low scan speed of 0.040° per second for optimal resolution. The peak intensities were measured for aragonite, HMC, LMC, and dolomite, and the presence of quartz was also recorded to provide a representative for terrigenous components within the sediment.

The program MacDiff 3.1.5 was then used to determine the amount of calcite and aragonite within the sediment by measurement of the total peak intensity, which is directly related to the peak area (Milliman, 1974). Calcite was composed of HMC and LMC, one forming the major peak and the other a minor peak on the shoulder of

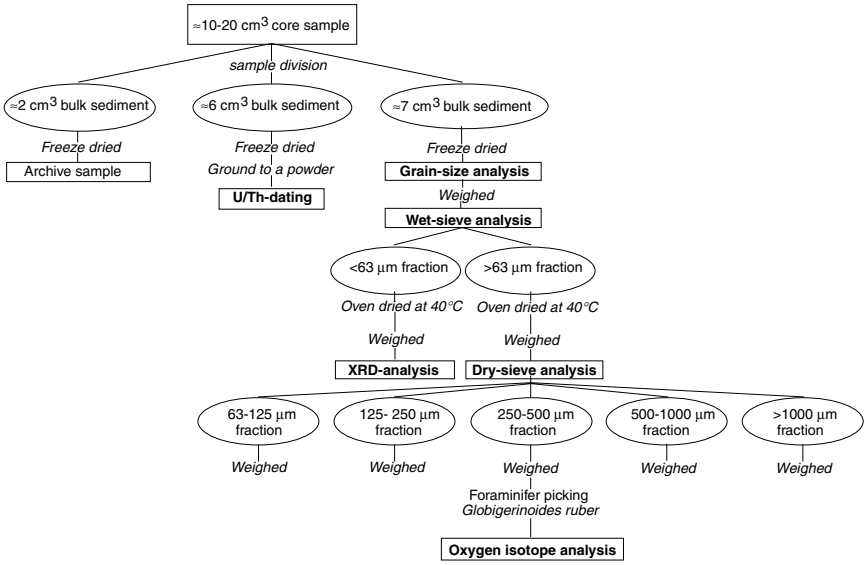

Figure 2. A flow diagram showing how the laboratory procedures were conducted. An initial division of the original sample into subsamples was made to provide sediment for a mineralogical analysis (X-ray diffraction), facies analysis (grain-size analysis), and stratigraphic analysis (oxygen isotope analysis and U/Th dating).

the major peak. The intensity of the major peak was measured and subtracted from the total calcite intensity to provide the intensity of the second (minor) peak. The relative weight percentage of calcite and aragonite were then calibrated using an "in-house" calibration curve formed from a series of measurements carried out on two component standards. These consisted of a laboratory-produced synthetic calcite and a pure aragonite from a Red Sea coral. The relative weight percentage of dolomite was then calculated using the linear correlation by Milliman (1974). The quartz data was left in peak-height intensities.

U/Th Dating

Thermal ionization U-Th analyses have been applied to sediment from four horizons in Site 1006 and six from Site 1003 (Henderson et al., Chap. 3, this volume). These horizons were selected from peaks in the interglacial aragonite stratigraphies to assign each package of aragonite-rich sediment to its correct highstand period. In general, U-Th dating of marine sediment is difficult because they contain appreciable amounts of initial 230Th bound in detrital clay minerals and scavenged from seawater. This initial 230Th gives the sediment a nonzero initial age and must either be removed or corrected for in order to arrive at a true age. The aragonite-rich sediments of the Bahamas are unusually high in U and low in initial Th so this problem is less acute than elsewhere (Slowey et al., 1996), but it must still be addressed. To reduce initial 230Th, analyses were performed on 63- to 250-μm pure-aragonite sediment separates. These procedures quantitatively remove the detrital material and reduce the concentration of scavenged Th. Remaining scavenged 230Th is corrected for by using the measured 232Th/230Th ratio and assuming a 232Th/230Th ratio for seawater. Full details of the sieving and heavy liquid protocols used for the separation and of blanks, chemical separation, and mass spectrometry can be found in Henderson et al. (Chap 3, this volume).

Sediment Flux Analysis

This procedure (Wolf and Thiede, 1991) consisted of freeze-drying 5-cm^3 bulk sediment samples in a vacuum container. The temperature was maintained at –40°C in liquid nitrogen. Dehydrated sample weights were taken using a digital scale (precision to 0.0001 g). Samples were then left to form a deflocculated suspension in distilled water prior to sieving.

Wet-Sieve Analysis

The 5-cm^3 suspensions were washed through a 63-μm metal sieve (U.S. standard) with a spray of distilled water. The coarse fraction (>63 μm) was drained and rinsed into 10-cm^3 containers for drying in fan-assisted ovens before weighing.

The fine fraction (<63 μm) was collected in large (5 L) beakers and left to settle. After settling, the water was siphoned off and the fine fraction was dried in fan-assisted ovens before weighing.

Dry-Sieve Analysis

The dried, weighed coarse fraction (>63 μm) was subsequently split (using a hand-held sieve set) into five subfractions: 63–125 μm, 125–250 μm, 250–500 μm, 500–1000 μm, and >1000 μm (U.S. Standard) (Fig. 3). Subfractions were stored in preweighed glass vials and their weights were measured.

RESULTS

Stratigraphy

Stratigraphy for the proximal site, Site 1003, and the distal site, Site 1006 (see Kroon et al., Chap. 2, this volume) is based primarily on oxygen isotope analyses and aragonite stratigraphy. Further age control is provided by U/Th-TMS-dating (Henderson et al., Chap. 3, this volume), and by nannofossil data (T. Sato, unpubl. data).

U/Th Dating

U-Th analyses confirmed that the uppermost aragonite-rich sediment package at both sites is Holocene and indicated that the next deepest package at Site 1006 was from the marine oxygen isotope Stage (MIS) 5 (Fig. 3). Samples from deeper in the cores had suffered perturbation of their U-Th system involving two processes. Samples have gained small amounts of U, probably because of transport of U downward in the sediment from oxidizing conditions into more reducing conditions where the U is insoluble. Samples have suffered progressive loss of 234U because of alpha recoil from the U-rich aragonite grains. These two processes prevent assigning accurate ages to the samples. However, given the fact that all samples were selected from high aragonite horizons and are, therefore, expected to be from sea-level highstands, the diagenetic perturbation can be sufficiently

well understood that each sample can be assigned to a unique interglacial event. A full discussion of this diagenesis and the rationale for its correction lies outside the scope of this paper but is presented in Henderson et al. (Chap. 3, this volume). The interglacials assessed from this U-Th analysis are marked on Figures 3 and 4 as their equivalent MIS. Those for Site 1006 are in good agreement with other age data (Kroon et al., Chap. 2, this volume). Those for Site 1003 differ somewhat from biostratigraphic age information and suggest a marked hiatus between the upper sediment package (MIS 1), and the package beneath it (MIS 11). Such a hiatus would explain the offset in $\delta^{18}O$ values seen at this depth in the sediment.

Oxygen Isotopes

Hole 1006A

Hole 1006A was chosen to provide an independent indicator of sea-level variations because of its greater pelagic component and its continuous record, which would increase its potential to provide a relatively complete age model. The validity of this age model is discussed further in the paper by Kroon et al. (Chap. 2, this volume). An almost complete (missing isotope Stage 7), high-resolution record extending to isotope Stage 44 was produced (Fig. 3). Good cyclicity within the isotope curve and a classic "sawtooth" profile is exhibited. The calcareous nannofossil bioevents constrain the assignment of the isotope Stages 8, 12, 22, 30, and 34 which are defined by *Emiliania huxleyi, Pseudoemiliania lacunosa, Reticulofenestra asanoi, Gephyrocapsa parallela,* and *Reticulofenestra asanoi*, respectively (Fig. 3) (T. Sato, unpubl. data). The U/Th dates provide further reinforcement defining the interglacial Stages 1, 5, 9, and 11 (Fig. 3) (Henderson et al., Chap. 3, this volume). The isotopic signal fluctuates between positive and negative values, which correspond to glacial and interglacials, respectively (Fig. 3). This cyclicity in the isotope record is replicated in the aragonite curve where drops in the percentage of aragonite correspond to the positive isotope values (i.e., glacials). It should be noted, however, that a slight offset is observed between the oxygen isotope and aragonite curves (indicated by the tie lines that are not horizontal; Fig. 3). This lag time indicates that the glacial maxima occurs later in the aragonite curve for some isotope Stages (e.g., 12–44) and before the maxima seen in the isotope curve for others (e.g., Stage 10 to the present). This displacement is by one or two samples or 20–40 cm. In the upper section of the core, above isotope Stage 12, the frequency of the isotope curve is lower and the isotope record shows the lightest isotope values, which are >–1‰ for the interglacial isotope Stages 1, 5, 9, and 11.

Hole 1003A

The interpretation given to the isotope curve at Site 1006 was used to help determine the age of the sediment at the more proximal hole (Hole 1003A), where the data lacks the classic sawtooth profile familiar to many deep-sea oxygen isotope records (e.g., Shackleton and Opdyke, 1973; Emiliani, 1978) (Fig. 4). Calcareous nannofossil bioevents and U/Th dates were once again used to constrain the assignment of the isotope stages. *E. huxleyi* and *P. lacunosa* define isotope Stages 8 and 12; however, the next nannofossil datum (*R. asanoi*) at isotope Stage 22 lies at a depth beyond the scope of this work (Fig.

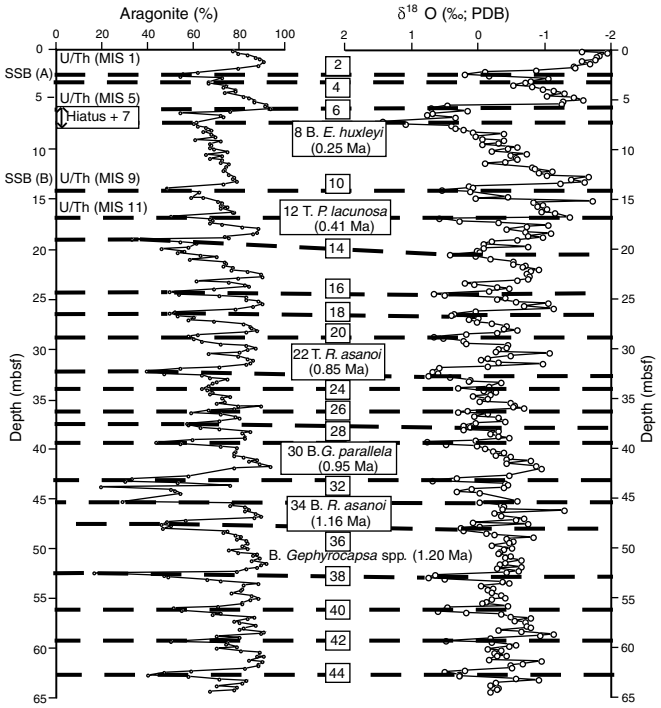

Figure 3. Comparison of the relative percentage of Aragonite in the fine fraction (<63 µm) with the planktonic foraminifer oxygen isotope stratigraphy for Site 1006 (Hole 1006A). The broken lines indicate the ties between the two records, and the numbers given to the lines depict the even (glacial) isotope stages. The position of the seismic stratigraphic boundaries (SSBs), calcareous nannofossil bioevents, and the U/Th dates are also marked. The U/Th dates are given as marine oxygen isotope stages (MIS). For details of how they were assigned to the raw U/Th dates see Henderson et al. (Chap. 3, this volume). PDB = PeeDee belemnite standard.

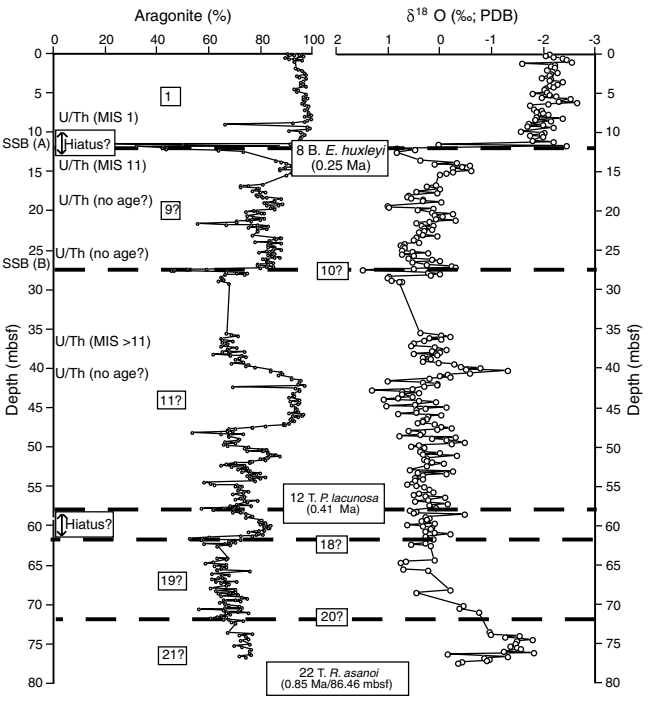

Figure 4. Comparison of the relative percentage of Aragonite in the fine fraction (<63 µm) with the planktonic foraminifer oxygen isotope stratigraphy for Site 1003 (Hole 1003A). The broken lines indicate the ties between the two records, and the numbers given to the lines depict the even (glacial) isotope stages. In addition, the position of the seismic stratigraphic boundaries (SSBs), calcareous nannofossil bioevents, and the U/Th dates are marked. The U/Th dates are given as marine oxygen isotope stages (MIS). For details of how they were assigned to the raw U/Th dates see Henderson et al. (Chap. 3, this volume). PDB = PeeDee belemnite standard.

4). Of the five samples measured using U/Th-dating, only the upper two lie within the U/Th methods limits of ~450 k.y. (Henderson et al., Chap. 3, this volume). These two samples define the interglacial Stages 1 and 11, implying that the interglacial Stages 3–9 are missing (Fig. 4). However, the lower U/Th-date assigned to isotope Stage 11 lies within the core section, which is isotopically heavy. Its accuracy could, therefore, be questionable, particularly because three of the lower U/Th measurements provide no ages and the fourth gives a value older than the measurement limits of U/Th dating (Fig. 4). The upper 12 mbsf of this core has an isotopic signal that fluctuates about –2‰. At 12 mbsf, there is a sharp shift to +1‰, which marks a glacial period and the base of the Holocene sediment wedge. The nannofossil bioevents assign the sediment at 12 mbsf to isotope Stage 8, as indicated by the presence of *E. huxleyi* (T. Sato, unpubl. data). This indicates the presence of a large hiatus at this depth (Fig. 4). Below, the remainder of the record becomes isotopically heavy, with low-amplitude fluctuations around +0.5‰. However, at 19 and 27 mbsf, slightly higher amplitudinal changes occur. With the aid of the aragonite curve and nannofossil datum, we established a stratigraphic record that reaches isotope Stage 21. Another hiatus below isotope Stage 12 is present that is marked by the top of *P. lacunosa* (57 mbsf).

Mineralogy

The abundances of aragonite, HMC, LMC, and dolomite are representative of the fine fraction (<63 µm). The percentages are calculated for their relative concentrations within the calcium carbonate fraction. The trends described are based on the average percentages for the extreme values within the glacials and interglacials.

Hole 1006A

At Hole 1006A, the cyclicity shown in the aragonite curve is mirrored in the LMC curve (Fig. 5). The dominant mineral at this site is aragonite, which represents ~86% of the carbonate phase during interglacial times and 48% during glacials (Figs. 6B, 6C). This shows that although the maximum input of aragonite occurs constantly during interglacials, its production and deposition on the platform is not entirely switched off during glacials. Most of the remaining mineral assemblage in the carbonate phase is represented by calcite, primarily LMC, which forms 11% of the carbonate phase during interglacials and 41% during glacials (Figs. 6B, 6C). Thus, the reverse pattern of that in the aragonite curve is seen and maximum LMC input occurs during the glacials. Although HMC represents the smallest concentration of the calcite phase (~3% during interglacials and 5% during glacials), it occurs predominantly in the upper 17 m (isotope Stage 12 to the present) (Fig. 5). Below this depth, the intensity of HMC diminishes and appears only sporadically, whereas the LMC concentration shows a continued increase with depth downcore. The dolomite curve indicates an almost total absence down to 37 mbsf (isotope Stage 28) although its first appearance is at 17 mbsf (isotope Stage 12), where it represents <1% of the carbonate phase (Fig. 5). At 18 mbsf (isotope Stage 14), it forms 33% of the total carbonate phase. Below this it only appears sporadically in very low concentrations down to 37 mbsf, below which its occurrence increases with depth downcore. Dolomite concentrations are generally <1% during interglacials, and average ~6% during glacials (Figs. 6B, 6C). Quartz shows average peak-height intensities of 250 with maximum intensities during glacials, following a steady increase during the intergla-

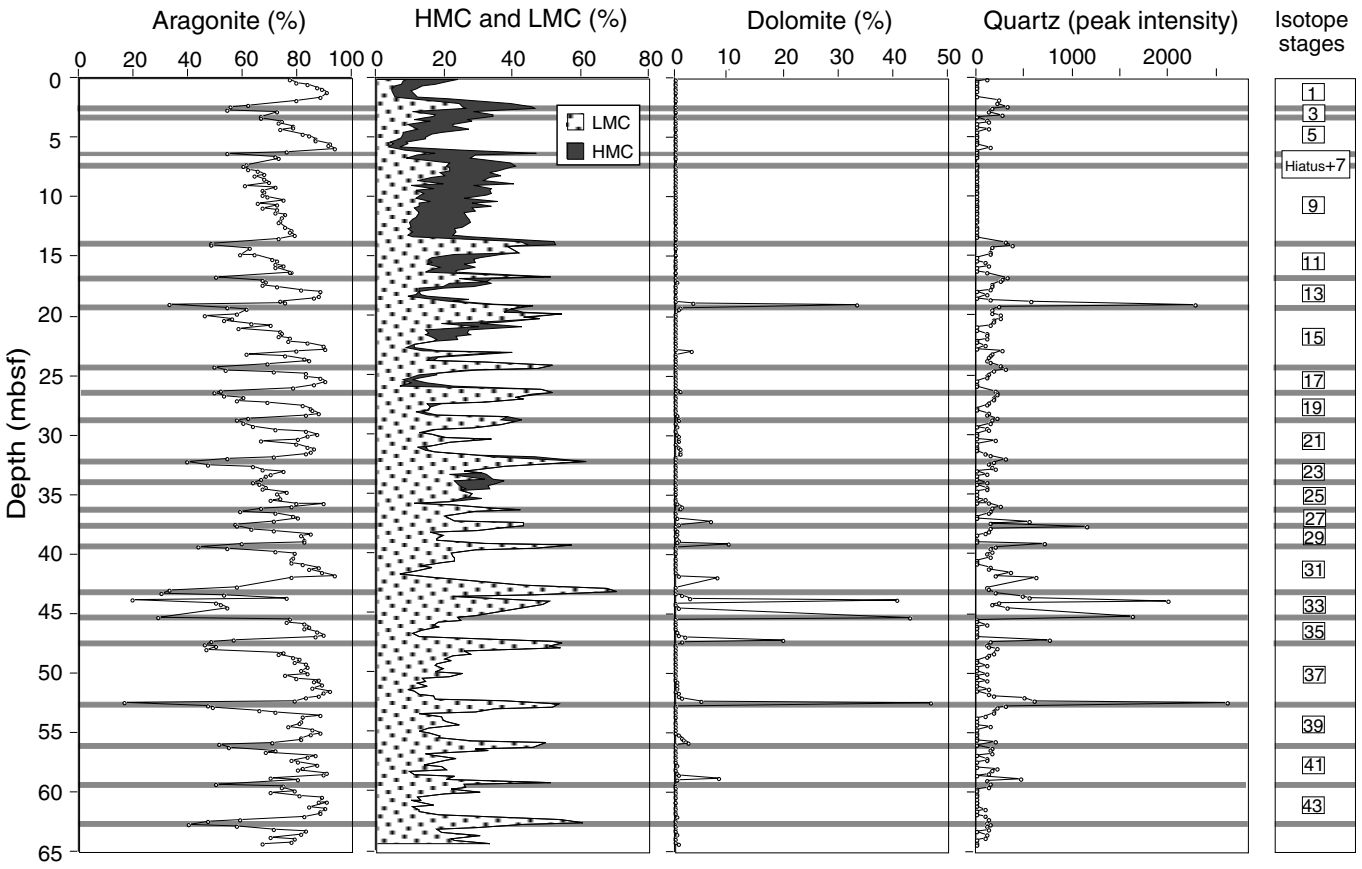

Figure 5. Downcore variations in the relative percentage of Aragonite, high-magnesium calcite (HMC), low-magnesium calcite (LMC), and dolomite for the fine fraction (<63 µm) for Site 1006. Downcore variations in the presence of quartz are given as peak intensity. The grey lines indicate the ties between the records and represent the glacial periods. The isotope stages are also shown, with the odd numbers indicating the interglacial periods (sea-level highstands).

cials after an almost total or total absence at the onset of the interglacials (Fig. 5). However, quartz appears only a few times, with very low intensities in the upper part of the core (down to isotope Stage 10), below which it shows a continuous presence downcore. Thus, it shows a similar trend to that seen in the LMC curve with highest concentrations during the glacials.

Hole 1003A

At Hole 1003A, clear variations occur within the carbonate phase (Fig. 7). Aragonite is the dominant mineral in the succession with an average concentration of 85% during the interglacials and 58% during glacials (Figs. 6E, 6F). Distinct decreases in aragonite content are observed at 12, 17, 21, 27, 48, 54, 57, and 62 mbsf. These decreases most likely represent cool periods or glacials. The remainder of the sediment in the calcium carbonate fraction is made up of LMC and HMC. LMC represents the largest portion with maximum concentrations during the glacials (29%) (Figs. 6E, 6F). HMC, although in lower concentrations forms 2% during the interglacials and 13% during the glacials (Figs. 6E, 6F). Both calcite minerals therefore favor the glacials. Dolomite is in very low concentrations (average <1%) at this site and represents 0%–2.5% of the carbonate fraction (Fig. 7). It is absent down to 17 mbsf, below which it increases at regular intervals with depth downcore. It shows a tendency (upcore) to occur directly after the maximum LMC and minimum aragonite concentrations, and shows a gradual depletion in concentration with continued high aragonite input (Fig. 7). At ~57 mbsf, dolomite generally increases in abundance downcore to 72 mbsf. Quartz appears, with low intensities, at 12 and 57 mbsf which correspond to isotope Stages 8 and 12, respectively.

Grain Size

Grain-size analysis is based on the subdivision of the sediment into subordinate grain-size fractions equivalent to the Udden-Wentworth grain-size classification of terrigenous sediments (Wentworth, 1922). This includes an initial division of the sediment into its coarse (>63 µm) and fine (<63 µm) components, which separates the silts and clays from the sand-sized sediment. Then five subsequent divisions of the coarse fraction separate the sediment into very fine sand (63–25 µm), fine sand (125–50 µm), medium sand (250–500 µm), coarse sand (500–1000 µm), and very coarse sand, granules, pebbles, and larger (>1000 µm). The trends described are based on average percentages derived from the extreme values within the glacials and interglacials.

Grain size has been used as a fundamental attribute of siliciclastic sedimentary rocks and, therefore, is one of the most important descriptive properties of such rocks, along with grain shape and fabric (Boggs, 1987). However, little is documented about these properties for carbonate rocks. These parameters together form the sedimentary texture that is produced primarily by the physical processes of sedimentation and, therefore, is thought to reflect sedimentation mechanisms and depositional conditions. It is the interrelationship of these primary textural properties that controls other derived textural properties such as bulk density, porosity, and permeability. Thus, grain-size distribution and sorting might also steer the fluid flow through the sediments and, therefore, combined with the mineralogy, affect the development of the initial diagenetic pattern. Extensive recrystallization or other diagenetic changes that may follow could destroy these original textures producing textural fabrics that are largely of secondary origin. Although much uncertainty still exists in the genetic interpretation of such textural data, a thorough understanding of the nature and significance of sedimentary textures is fundamental to the interpretation of ancient depositional environments and transport conditions. And, although these relationships are known, the relationship between grain-size characteristics and depositional environments is still little understood. Thus, here we document grain-size variations through both time and space to provide further insight into the importance of grain size as an aid to our understanding the sedimentary environment and as a proxy for stratigraphic work.

Hole 1006A, Bulk Sediment

At Hole 1006A, the first important observation is that the sediment at this site is dominated by the fine fraction (Fig. 8), which on average forms ~75% of the sediment (Fig. 9A). Fluctuations in the amount of fine fraction occur at regularly spaced intervals downcore that switch from high concentrations of fine fraction to higher con-

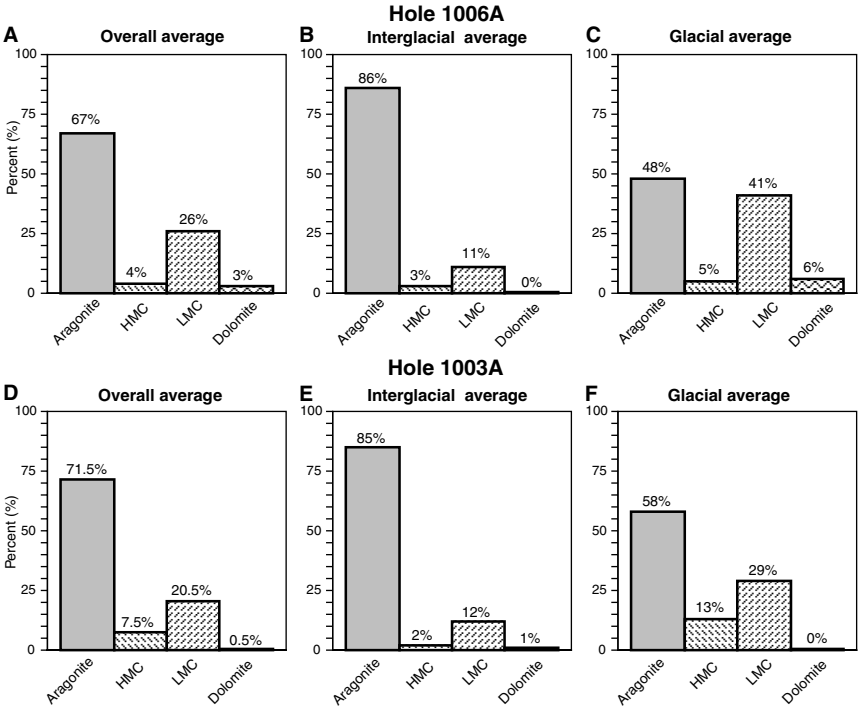

Figure 6. Trends in the relative percentages of the carbonate mineralogy for the fine fraction (<63 µm) at the distal site (Hole 1006A) and the proximal site (Hole 1003A). Histograms **A** and **D** show the overall (interglacial and glacial combined) average mineralogical trends for Hole 1006A and Hole 1003A, respectively. Histograms **B** and **E** show the interglacial trends, whereas histograms **C** and **F** show the glacial trends for each of the holes. These trends are based on averages for the extreme values in both the interglacial and glacial periods.

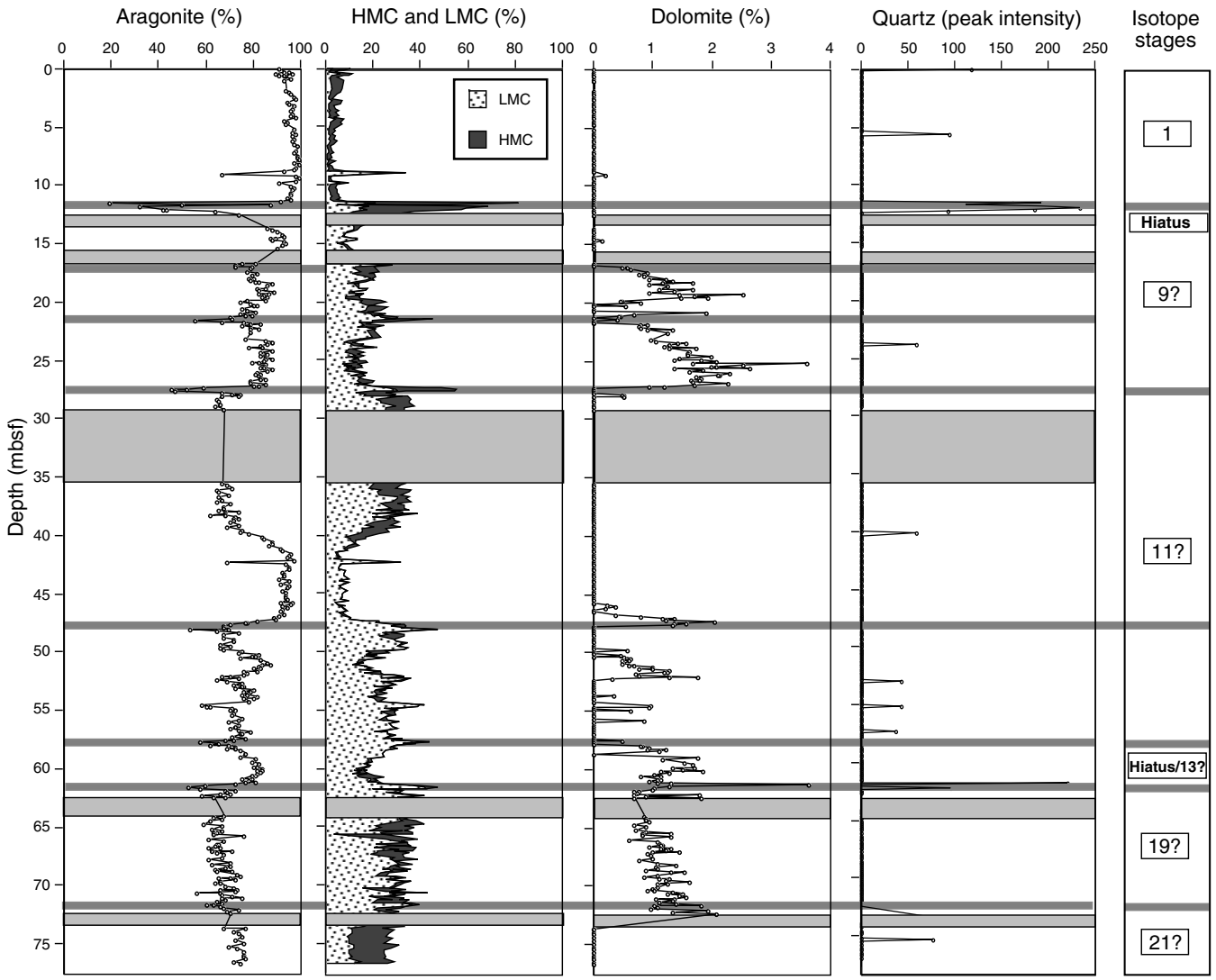

Figure 7. Downcore variations in the relative percentage of aragonite, high-magnesium calcite (HMC), low-magnesium calcite (LMC), and dolomite for the fine fraction (<63 µm) for Site 1003. Downcore variations in the presence of quartz are given as peak intensity. The blocked grey areas represent gaps in the record, and the grey lines indicate the ties between the records and the glacial periods. The isotope stages are also shown, with the odd numbers indicating the interglacial periods (sea-level highstands).

centrations of coarse fraction (Fig. 8). If we look at these switches we can see that the sediment during interglacials is dominated by the fine fraction, which forms on average 88% of the total sediment (Figs. 8, 9B). In the glacials however, although the fine fraction is still the dominant grain size, forming 62% of the sediment, the coarse fraction is much more important here, forming 38% of the sediment (Fig. 9C). Thus, although there is in general a dominance by the fine fraction, the biggest contrast between the glacials and interglacials exists in the coarse fraction (Figs. 9B, 9C). A final point of interest is the general increase in the percentage of coarse fraction in the upper part of the core which is represented by isotope Stage 9 to the present (Fig. 8).

Hole 1003A, Bulk Sediment

The trend observed at Hole 1006A is also seen at Hole 1003A (i.e., the sediment is dominated by the fine fraction [70%]) (Figs. 9D, 10). During interglacials, the fine fraction dominates and on average represents 86% of the sediment (Fig. 9E). In the glacials, although the fine fraction is still the dominant grain size (54%), this is only marginally so while the coarse fraction forms ~46% of the sediment (Fig. 9F). Therefore, there is again a sharp reduction in the coarse fraction input during interglacials and a relatively sharp increase during glacials. The increase in the coarse-fraction percentage at 17, 21.5, and 47 mbsf (Fig. 10) probably represents cool periods within the interglacials, possibly isotope Stages 8.6, 9.2, and 11.2, respectively. In addition, there is a marked increase in the concentration of the coarse fraction at 37 and 54 mbsf, and a general increase can be seen at 60 mbsf where, on average, it represents 35% of the total sediment (Fig. 10).

Hole 1006A, Coarse Fraction (>63 µm)

If we now look at the subdivisions of the total coarse fraction at the distal hole (Hole 1006A), the 63- to 125-µm fraction represents the highest proportion of the coarse fraction, representing 36% of the total sediment (Fig. 11). This is followed by the other subfractions that show a general decrease in input with increasing grain size (Fig. 12A). Thus, it is the very fine to medium sand fraction that dominates the coarse fraction. However, we find that during the interglacials the sediment is dominated by the 63- to 125-µm fraction (very fine sand

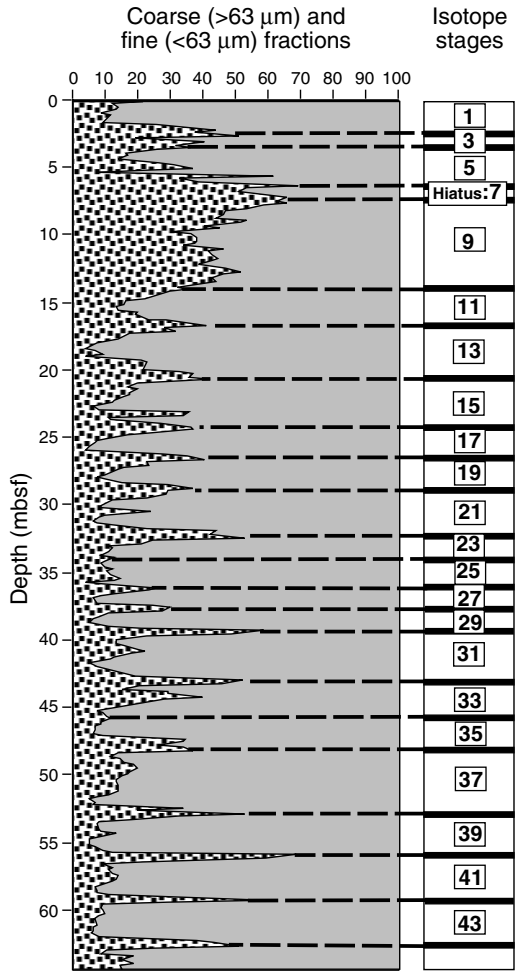

Figure 8. Downcore variations in the percentage of fine and coarse sediment at Site 1006. The dotted pattern represents the coarse fraction (>63 µm), and the grey pattern represents the fine fraction (<63 µm). The broken black lines tie the peaks to the isotopic "age" model. The numbers between the lines depict the odd (interglacial) isotope stages. The hiatus in the upper-core section is marked.

fraction), representing 50% of the total sediment (Fig. 12B), and that with each consecutive increase in grain size there is a decrease in input (Fig. 12B). In contrast, during the glacials the larger subfractions form a higher percentage of the coarse sediment (i.e., 250- to 500-µm fraction [28%], 500- to 1000-µm fraction [14%], >1000-µm fraction [18%]). These represent the medium to very coarse sand fractions (Fig. 12C). Thus, the interglacials show an increase in the two smallest subfractions and a decrease in the three larger subfractions when compared to the glacials (Figs. 13B, 13C). However, because the grain-size distribution pattern during interglacials exhibits decreasing input with increasing grain size (i.e., "normal sorting") (Fig. 12B), it must be the variations in the glacial trend (Fig. 12C) that influence the general pattern seen for the total coarse fraction (Fig. 12A).

Hole 1003A, Coarse Fraction (>63 µm)

At Hole 1003A, the patterns and concentrations seen in the subdivisions of the coarse fraction are slightly different from those seen at the distal site (Fig. 13). The 63- to 125-µm fraction again represents the highest proportion of the sediment (52%) while the second highest concentration is represented by the 125- to 250-µm fraction (21%) (Fig. 12D). Thus, it is once more the smallest subfractions that dominate the grain size of the coarse fraction. During the interglacials, the average percentages of the subfractions decrease with increases in the grain sizes from 71% for the 63- to 125-µm fraction to 2% for the >1000-µm fraction (Fig. 12E). This pattern is similar to that seen at the distal site during the interglacials. However, during the glacials, the order is slightly modified so that the >1000-µm fraction (very coarse sand fraction) represents the second largest percentage concentration within the coarse fraction (25%) while the 63- to 125-µm fraction (33%) is the most abundant (Fig. 12F). This is very different from that seen at the distal site. If we compare the percentages of the different grain sizes between the glacials and interglacials we find that, during the interglacials, there is an increase in the volume of the 63- to 125-µm fraction, while all the other fractions show a distinct decrease (Figs. 12, 12F). Therefore, as with Hole 1006A, the general grain-size distribution within the coarse fraction at Hole 1003A shifts remarkably going from an interglacial to a glacial and vice versa.

DISCUSSION

Stratigraphy

The $\delta^{18}O$ records for both sites along the leeward side of the Great Bahama Bank show that there have been numerous periods during the past 1.4 Ma where changes in sea level have occurred in response to climatic variability. In turn, the way in which the Bahama Platform has responded to these changes has been recorded in the mineralogy and grain-size distribution of the sediment. The $\delta^{18}O$ record for the distal hole (Hole 1006A) has shown that there has also been a general climatic warming during the late Pleistocene (after isotope Stage 11). This is indicated by the lightest $\delta^{18}O$ values that were interpreted as surface-water warming by Kroon et al. (Chap. 2, this volume). However, at the more proximal hole (Hole 1003A), this warming trend is more difficult to observe because of missing sequences in the stratigraphic record and an isotopically "heavy" record, which indicates diagenetic overprinting below the Holocene (>12 mbsf). This is marked by a 3‰ shift in the oxygen isotope values. A possible reason for this shift could be diagenetic overprinting caused by early diagenesis. This is supported by evidence found in the mineralogy, discussed later. Further discussion concerning the isotope curve at the distal site (Site 1006) in terms of its paleoceanographic and climatologic significance can be found in the paper by Kroon et al. (Chap. 2, this volume).

Mineralogy

It has been noted that the aragonite cycles at Site 1006 display the same sawtooth pattern as the $\delta^{18}O$ record, while at Site 1003 only the aragonite curve shows this pattern. However, the reason for this aragonite pattern is still under debate since the Bahama Bank has a flat-topped morphology; thus the aragonite variations should resemble a more "square wave" pattern (Droxler et al., 1983; Haddad and Droxler, 1996). It has been suggested that these unexpected differences between the predicted and actual aragonite patterns could be the result of seafloor aragonite dissolution (Droxler et al., 1983; Droxler, 1985). The idea for dissolution was first put forward by Lynts et al. (1973) as a potentially important factor controlling the periplatform carbonate mineralogy of the Great Bahama Bank. However, the two cores at Holes 1006A and 1003A were recovered at 658 and 481 mbsl respectively, and are, therefore, too shallow to adequately discuss possible changes that could result from seafloor aragonite dissolution. This seems to support the observation by Boardman and Neumann (1984) that stated that carbonate dissolution would not occur at shallow water depths (e.g., 200–2000 mbsl; Providence Channel, Bahamas) and that the aragonite content is solely an input signal. Within the periplatform ooze (Schlager and James, 1978), aragonite was found to be the most abundant mineral on the leeward side of the

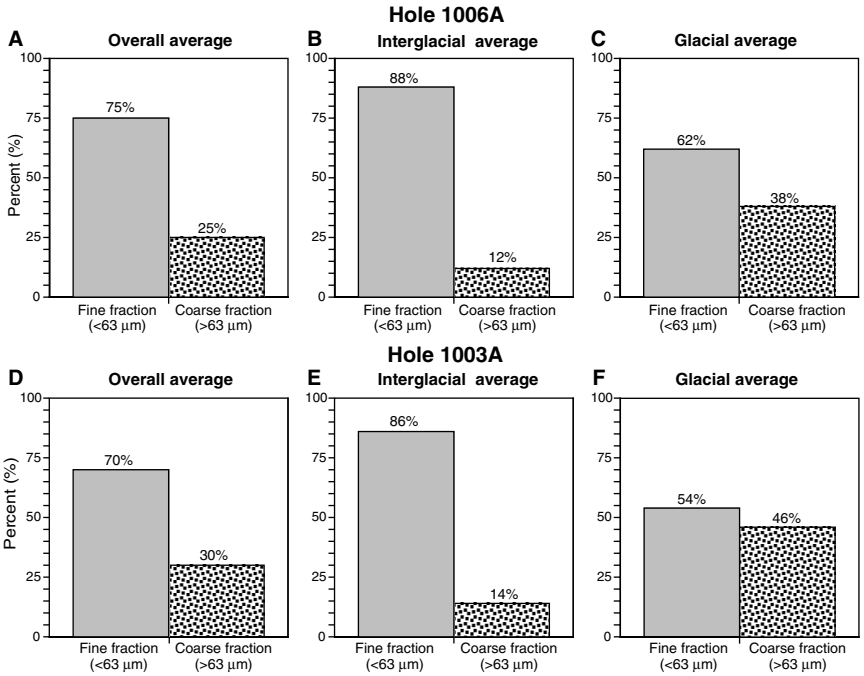

Figure 9. Trends in the relative percentages of the coarse (>63 μm) and the fine (<63 μm) fractions at the distal site (Hole 1006A) and the proximal site (Hole 1003A). Histograms **A** and **D** show the overall (interglacial and glacial combined) average grain-size distributions for Holes 1006A and 1003A, respectively. Histograms **B** and **E** show the interglacial trends, whereas histograms **C** and **F** show the glacial trends for each of the holes. These trends are based on averages for the extreme values in both the interglacial and glacial periods.

Great Bahama Bank. As known from literature, its main sources are neritic, bank-top aragonite needles and pelagic-derived pteropods (e.g. Neumann and Land, 1975; Droxler et al., 1983; Boardman and Neumann, 1984, 1986; Boardman et al., 1986; Macintyre and Reid, 1992; Milliman et al., 1993). However, a small decrease in the aragonite content of these periplatform sediments was found to occur with increasing distance and water depth from the platform top (Figs. 6A, 6D). Boardman and Neumann (1984) found a similar pattern for Northwest Providence Channel. These observations were also made for sediments from the Bahama Channels (Droxler et al., 1988; Reijmer et al., 1988; Haddad and Droxler, 1996) and the Bermuda Pedestal (Berner et al., 1976), as well as for the Nicaragua Rise (Droxler et al., 1991). If the decrease observed is solely the result of input variations or if minor diagenesis might have modified the signal remains to be seen (deMol et al., 1998). We found that, although this general off-bank decrease occurred, the general fluctuations in aragonite concentrations, coupled with the $\delta^{18}O$ records, indicate that aragonite is in its highest concentrations at both sites during sea-level highstands and in its lowest concentrations during sea-level lowstands (Fig. 6). This difference related to sea level also occurs in a spacial context. It seems that sediment deposited during sea-level highstands does not vary spatially between Holes 1003A and 1006A, but it is the lowstand concentrations that vary (Fig. 6). Therefore, with increasing proximity to the shallow-water platform realm, the difference between the highstand and lowstand aragonite concentrations is less pronounced (Fig. 6). For example, at the distal site (Hole 1006A), there was a 77% increase in aragonite concentration during sea-level highstands, whereas this difference was only 50% at the more proximal site (Hole 1003A). Thus, the decrease in the aragonite content of these periplatform sediments with increasing distance from the platform top seems to be controlled by changes within the aragonite content of the sediment deposited during sea-level lowstands. These results further support the idea that the aragonite signal is an input signal at these shallow depths and not a dissolution modified signal.

In the literature, it is described that HMC input occurs preferentially during interglacials and shows a positive correlation to aragonite (Boardman et al., 1986; Glaser and Droxler, 1993; Emery, 1996; Haddad and Droxler, 1996) or a negative correlation (Droxler, 1985, 1986). At both sites along the platform slope, HMC is in highest concentrations during glacials (e.g., 5% at Hole 1006A and 13% at Hole 1003A; Fig. 6) and, therefore, runs reverse to the aragonite input pattern. Grammer et al. (1993a, 1993b) demonstrated that, where botryoidal aragonite cements form on steep marginal slopes (Tongue of Ocean, Bahamas), discontinuity horizons exist that consist of thin layers of magnesium-calcite micrite. Similar observations were made at the Belize Barrier Reef (Ginsburg and James, 1976). If these then form part of the eroded slope debris that is deposited during glacials (see "Glacials" and "Grain Size" sections), this could account for the higher HMC concentrations in these intervals. In addition, as observed at Site 1005 (deMol et al., 1998), at CLINO and UNDA (Westphal, 1997; Westphal et al., 1999), and at the deep seafloor of Tongue of the Ocean (Schlager and James, 1978), HMC cements are formed during early diagenesis that would also increase its relative concentration, especially at the more proximal hole (Hole 1003A), where early diagenesis has been implied by the isotope curve. This would also account for the proximal site having higher HMC concentrations when compared to the distal site (i.e., a spacial discontinuity), whereby HMC decreases in concentration with increasing distance from the platform (Fig. 6). A final reason for this spacial discontinuity is that the more proximal site is closer to the source area of the magnesium-calcite micrite.

Along the leeward flanks of the Great Bahama Banks, LMC is found to be in highest concentrations during sea-level lowstands (e.g., 29% at Hole 1006A, and 41% at Hole 1003A; Fig. 6). The highstand shedding theory states that during sea-level lowstands there is relatively little neritic carbonate production and low aragonite content (Schlager et al., 1994; Droxler and Schlager, 1985; Haddad and Droxler, 1996). Thus, the sediments are dominated by pelagic input such as pelagic foraminifers and coccoliths that are high in LMC (Johnson, 1961; Scholle et al., 1983; Tucker and Wright, 1990). In addition, the lowstand deposits are dominated by coarse-grained, eroded, slope debris (see "Glacials" and "Grain Size" sections) which could contain lithified rock (i.e., calcite cements). During sea-level highstands, the LMC signal is diluted by the high influx of aragonite-rich sediment. However, this neritic input is drastically reduced during lowstands allowing the LMC signal to be relatively enriched during these periods. The spacial discontinuity in the concentration of LMC in the sediment shows that LMC increases preferentially with increasing distance from the platform, showing a negative correlation

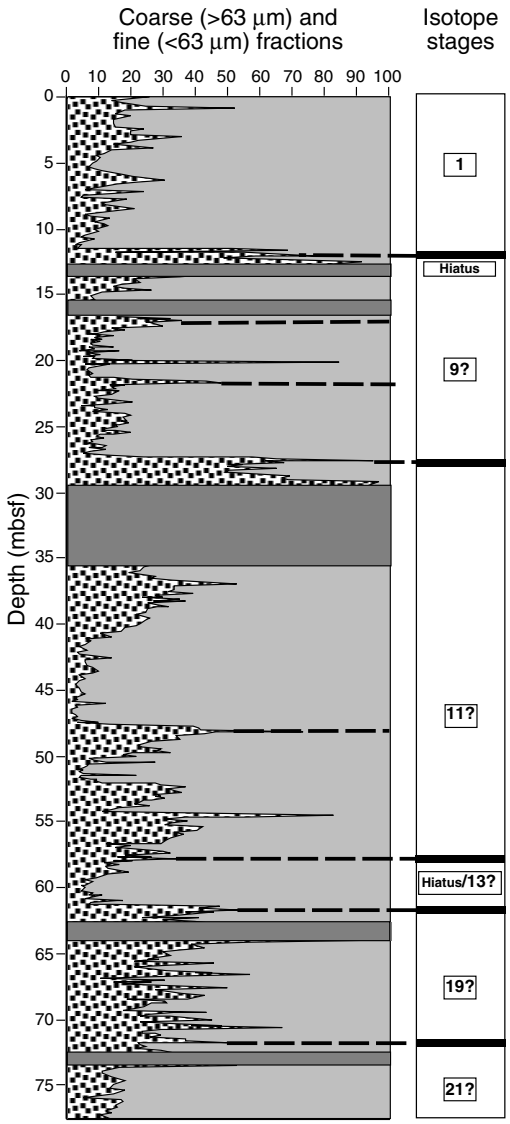

Figure 10. Downcore variations in the percentage of fine and coarse sediment at Site 1003. The dotted pattern represents the coarse (>63 µm) fraction, and the grey pattern represents the fine (<63 µm) fraction. The blocked grey areas represent gaps in the record. The broken black lines tie the peaks to the isotopic "age" model. The numbers between the lines depict the odd (interglacial) isotope stages. The hiatuses are also marked.

to the HMC (Fig. 6). For example, the average LMC concentration at Hole 1006A equates to 26%, compared to only 20.5% seen at Hole 1003A (Fig. 6). This is probably connected to the pelagic input, which increases with increasing distance from the platform. This would also account for the difference between the interglacial and glacial concentrations at the distal site being greater than that seen at the proximal site (Fig. 6).

Dolomite, as a whole, shows very little relationship to the other carbonate minerals. However it does show some trends in terms of glacial/interglacial interplay and spacial variations. At both sites, the first appearance of dolomite is at 17 mbsf, which implies that its presence could be depth dependent; however, that is where the similarity ends. It appears during sea-level lowstands at Hole 1006A, thereby showing a positive correlation to LMC, HMC (Fig. 6), and also to quartz, which appears during these periods. Because quartz represents terrigenous material, this suggests that the dolomite could be of detrital origin. This was also seen in Hole 632A of ODP Leg 101 on the windward side of the Great Bahama Bank (Reijmer et al., 1988). In contrast, at Hole 1003A, dolomite appears in almost every sample from isotope Stage 9 down (with the exception of the upper part of isotope Stage 11 (11.1)), which suggests that its formation is caused by early diagenesis (Mullins et al., 1985). Droxler et al. (1988) and Reijmer et al. (1988) observed a similar pattern. Quartz at the proximal site only appears at two intervals that correspond to sea-level lowstands (isotope Stages 2 and 12).

Grain Size

Sediments from different environments tend to have distinctive grain-size characteristics. The ultimate characteristic of the sediment grain-size distribution is a function of several interacting processes, beginning with growth/production and subsequent erosion in the source area. Thus, the ultimate size distribution of grains in the site of deposition is a function of (1) availability of grains of different sizes at the source, (2) transport and depositional processes, and (3) postdepositional diagenetic changes (Boggs, 1987). To date, the majority of research into grain-size analysis has been based in siliciclastic environments. In carbonate environments, grain size usually only classifies the sediment broadly using terms which combine grain type and depositional texture (e.g., boundstone, grainstone, packstone, etc. [Dunham, 1962]). Therefore, we have attempted to look at the grain-size distribution to provide further insight into its importance as a proxy to aid in understanding the carbonate sedimentary environment. Although this may be relatively premature, we find that it is possible to use grain-size characteristics as "fingerprints" of certain environments. In the carbonate regime, the highest, most variable off-bank sediment transport occurs during interglacials (sea-level highstands), as shown by numerous authors like Mullins (1983), Droxler and Schlager (1985), Reijmer et al. (1988), and Eberli, Swart, Malone, et al. (1997), whereas evidence for low sedimentation rates during glacials was shown by Kendall and Schlager (1981) and Handford and Loucks (1993). Emery and Myers (1996) stated that in both siliciclastic and carbonate environments this variability in sedimentation rate between interglacials and glacials is probably caused by gravity-controlled sedimentation, rather than by a uniform, continuous rain of pelagic sediment. The grain size results will show that this is true for the glacials, but not the interglacials.

Although we find that both sites on the leeward side of the Great Bahama Bank are dominated by the fine fraction (<63 µm), there is some spacial variation (Figs. 9A, 9D). Furthermore, the difference in the percentage of coarse to fine sediment is greater at the distal site than at the proximal site, which indicates that less coarse-grained sediment is deposited at the distal site, thus confirming dominance by the fine fraction. These spacial variations could be related to the site locations in relation to their position on the leeward side of the Great Bahama Bank.

On windward margins of carbonate platforms, wave activity tends to push most of the fine sediment onto the platform, leaving the coarser fraction to accumulate on the windward side (e.g. Emery and Myers, 1996). Hine et al. (1981a, 1981b) and Tucker (1985) found that accumulation of the finer sediment tends to occur on the leeward margins. The large-scale westward progradation of the Great Bahama Bank as shown by Eberli and Ginsburg (1989) and Eberli, Swart, Malone, et al. (1997) demonstrates this sedimentary process. Similar observations were made for the Devonian Iberg Reef (Gischler, 1995), Pedro Bank (northern Nicaragua Rise; Glaser and Droxler, 1993) and the Queensland Plateau (northeastern Australia; Betzler et al., 1995). The fine-fraction dominance at both sites (Figs. 9A, 9D) confirms these observations. The proximal site lies on the slope, which forms a progradational wedge, whereas the distal site is located more basinward in the Santaren Channel. This progradational phase of the platform described by Eberli and Ginsburg (1987), Wilber et al. (1990), and Eberli et al. (1994) was found to contain a high concentration of fine (<63 µm) aragonite needles, which, although originating from

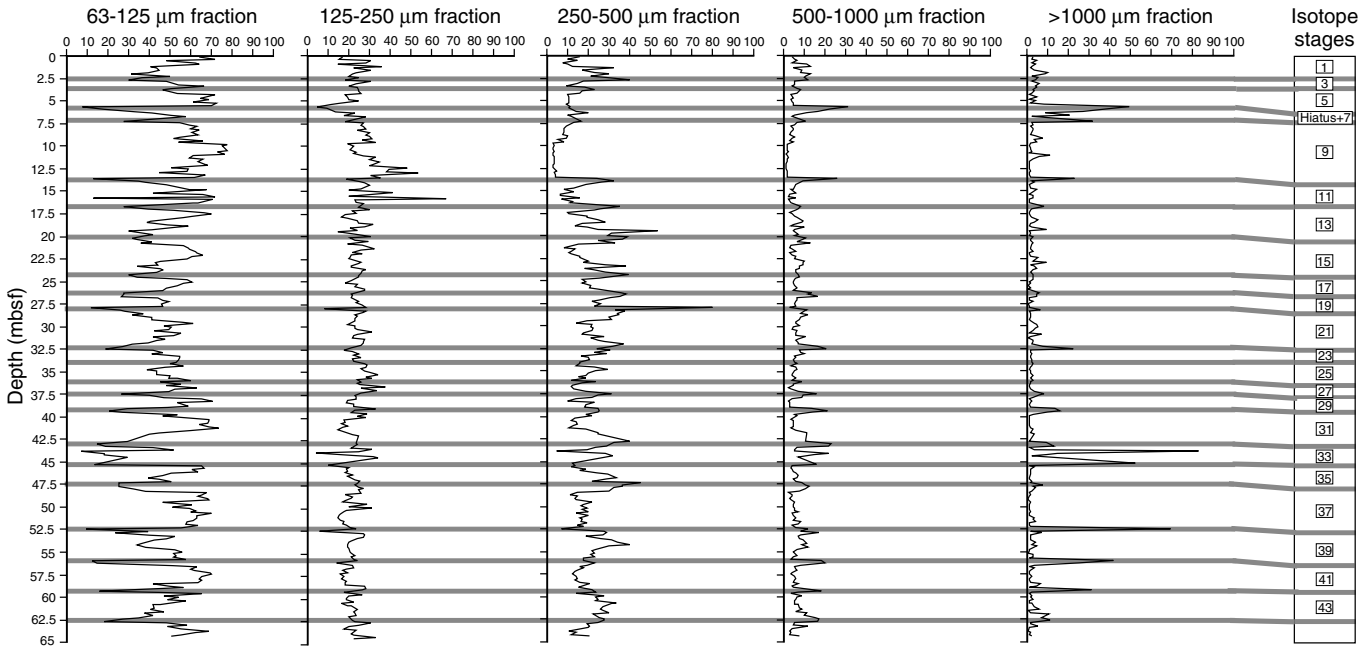

Figure 11. Site 1006 variations in the distribution of the subfractions within the coarse-grained sediment (>63 µm), which is subdivided into five component sizes. The grey tie-lines indicate the positions of the even (glacial) isotope stages and are connected to the isotope "age" model, which is based on the $\delta^{18}O$ data (the odd numbers given represent the interglacial periods). Note that there is a slight depth difference (lag time) between the positions of the isotope stages when comparing the grain-size data with the $\delta^{18}O$ data.

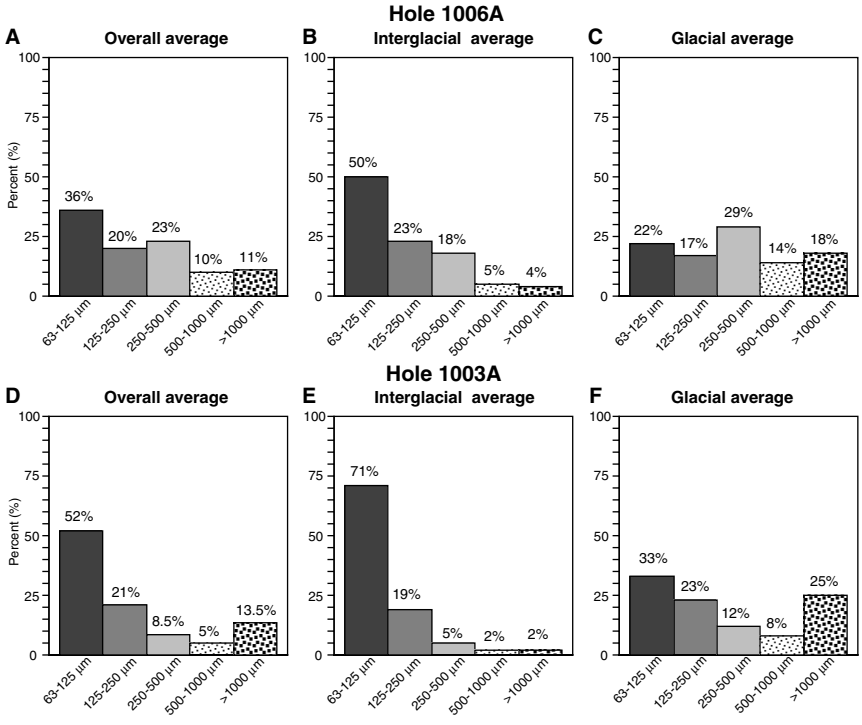

Figure 12. Trends in the relative percentages of the coarse fraction (>63 µm) subdivisions; very fine sand (63–125 µm), fine sand (125–250 µm), medium sand (250–500 µm), coarse sand (500–1000 µm), and very coarse sand, and pebbles (>1000 µm). Histograms **A** and **D** show the overall (interglacial and glacial combined) grain-size distributions for the distal site (Hole 1006A) and the proximal site (Hole 1003A), respectively. Histograms **B** and **E** show the interglacial trends, whereas histograms **C** and **F** show the glacial trends for each of the holes. These trends are based on averages for the extreme values in both the interglacial and glacial periods.

the platform top, can nevertheless be deposited well into the basin (Wilber et al., 1990; Droxler et al., 1991; Glaser and Droxler, 1993; Milliman et al., 1993). In other words, the sediment grain sizes supplied to the slope are dependent on the orientation of the slope with respect to the wind regime. Depending on their velocity and their position within the basin, surface and bottom currents might modify this input signal (Mullins et al., 1980).

Work carried out by Kenter (1990) researched the relationship between slope angle and dominant sediment fabric. The resultant model showed that coarse-grained sediment could maintain much higher angles of repose and hence steeper slopes than fine-grained deposits. Thus, at Site 1003 where the slope angle is low (= 3.5°), fine-grained mud would be the representative sediment type. This environment is also characterized by reorganization of the slope deposits that could

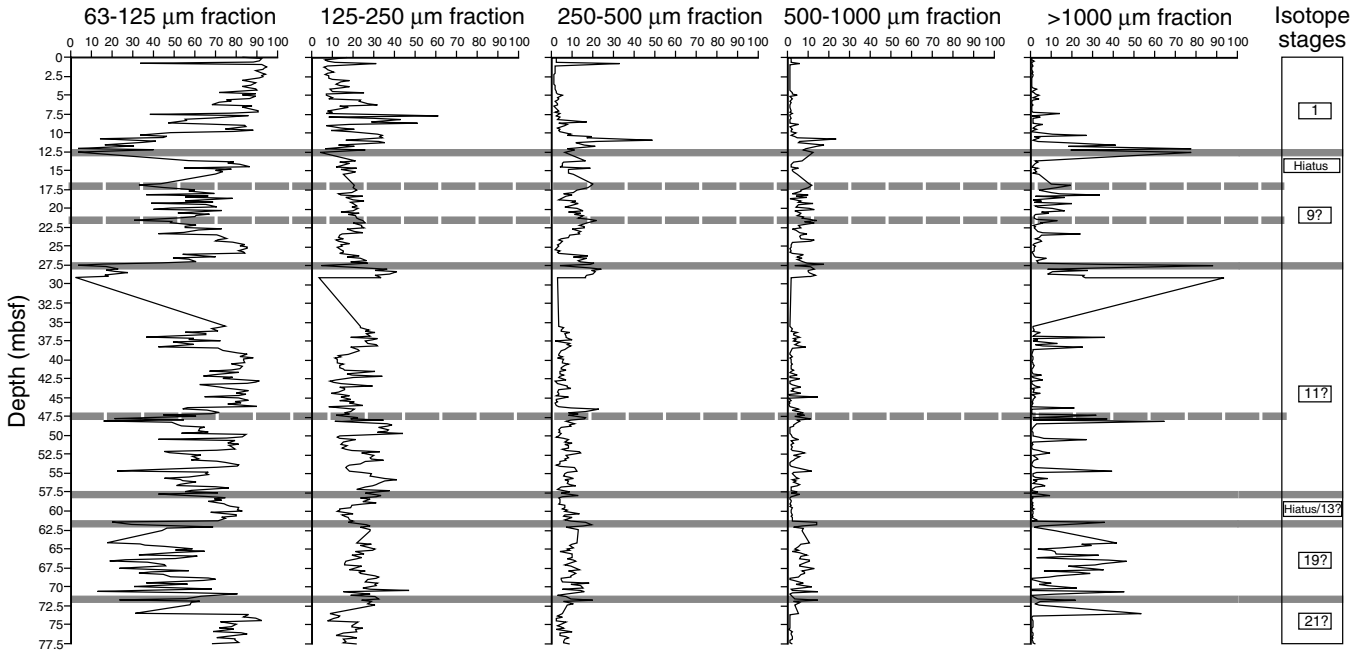

Figure 13. Site 1003 variations in the distribution of the subfractions within the coarse-grained sediment (>63 µm), which is subdivided into five component sizes. The solid grey tie lines indicate the positions of the even (glacial) isotope stages, and the broken grey tie lines indicate possible subdivisions of the stages. Both sets of tie lines connect the data to the isotope "age" model, which is based on the $\delta^{18}O$ data (the odd numbers represent the interglacials). The gaps in the record are not marked here so that the fluctuations in the graph can be seen clearly.

explain the observed hiatuses seen at this proximal site. The slightly marked increase in the average percentage concentration of fine fraction (Fig. 9A) and the decrease in slope angle at the distal site could be the result of higher pelagic input of fine-grained material compared to the steeper slope and coarser grained deposits seen at the proximal site (Fig. 9D). The high percentage of aragonite of these deposits, however, points to a more platform-related input pattern. The dominance of the fine fraction at the basinal site could result from (1) resedimentation of fine-grained sediment originally deposited at the slope, (2) the fine end-tails of platform-derived turbidites, or (3) result from normal off-bank transport (Wilson and Roberts, 1995).

Interglacials

During the interglacials or sea-level highstands, the proportions of fine (<63 µm) to coarse (>63 µm) sediment seen at both sites (Holes 1006A and 1003A) are very similar (Figs. 9B, 9E). This is probably caused by large export of aragonite-rich muds from the platform top by "density cascading," whereby waters are released from the platform together with entrained sediments that later fall out of suspension as pelagic rain to form "pelagic draping" of the slope and basin (Wilson and Roberts, 1995). In addition, even though the coarse fraction forms the smallest percentage concentration of the sediment (Figs. 9B, 9E), normal sorting occurs within this fraction so that with increases in the grain size there is a decrease in percentage concentration of each consecutive grain-size subdivision (Figs. 12B, 12E). This indicates that all grain sizes are being eroded from the platform top and transported downslope to be deposited across the entire platform-to-basin transect during sea-level highstands and that sorting increases with increasing distance from the source. Therefore, the differences seen in the average coarse/fine grain-size distribution (Figs. 9A, 9D) and within the coarse-fraction subdivisions for the two sites (Figs. 12A, 12D) is solely effected by the volume of the coarse fraction (>63 µm). In addition, Westphal (1997) found that fine-grained, highstand slope sediments from the Great Bahama Bank (the CLINO Core) were protected against large initial fluid-flow alterations because of their low permeability, and thus were subjected to less diagenetic alteration. Therefore, diagenesis within these deposits, as well as being affected on a vertical scale (i.e., through time), is also affected spatially (if to a lesser extent) so that with increasing distance from the platform, and thus decreasing grain size, the diagenetic potential of the sediment is reduced.

Glacials

When considering the glacial sediments deposited during sea-level lowstands, it was observed that the coarse fraction (>63 µm) constituted 38% of the sediment at the distal site and 46% of the sediment at the proximal site (Figs. 9C, 9F). Thus, the concentration of the coarse fraction is of greater significance at both sites during sea-level lowstands. Mullins et al. (1980) showed that maximum bottom-current strengths in the Straits of Florida correlate with glacials. They propose that the system responds to compressed worldwide climatic belts and increased wind regimes, which intensify ocean circulation during these times. The pattern in the grain-size distributions observed in our cores is in full agreement with these observations. Glaser and Droxler (1993) found a similar pattern for the Walton Basin north of Pedro Bank. However, there is a change in the coarse/fine proportions across the platform during glacials that was not so prominent during the interglacials. This decrease in coarse fraction from the proximal to distal site during the glacials is caused by the types, frequencies, and strength of the mechanisms that transport the sediment away from the platform. Normally, with increasing distance from the source, these gravity-induced transport mechanisms lose energy and are unable to support the larger particles in suspension, thus depositing them nearer to the platform (e.g. Boardman and Neumann, 1984; Boggs, 1987). This would account for the reduced concentration of both the bulk coarse fraction (Fig. 9C) and the larger subfractions (Fig. 12C) at the distal site, which is supported by the reduced input of turbidites at this site (Eberli, Swart, Malone, et al., 1997). Another important point is that carbonate systems do not experience the same type of physical erosion as seen in siliciclastic environ-

ments. For example, subaerial exposure of the carbonate platform top will tend to cause chemical erosion, resulting in grain and cement dissolution and reprecipitation of dissolved material (Emery and Myers, 1996). Westphal (1997) found that these coarse glacial deposits, with their higher permeabilities, were subjected to intense diagenetic alteration. They also contained high HMC cements which, together with the eroded slope deposits containing magnesium-calcite micrite (Grammer et al., 1993a, 1993b), would explain the high HMC concentrations during sea-level lowstands. Diagenesis would once again be effected spatially in the same way as during interglacials (i.e., the diagenetic potential of the sediments would be reduced [not to the same degree] with distance from the platform.).

The facies distribution pattern of the Great Bahama Bank of Purdy (1963) clearly showed the grain-size differences across the platform top. Relatively coarse-grained sediments are found at the platform edge, both on the windward and leeward side, whereas mud-size sediment dominates the platform interior facies. Thus, flooding and exposure of the platform will introduce variability in the grain sizes that can be produced and subsequently exported. Dravis (1996) clearly demonstrated that fresh-water calcite cementation will rapidly freeze platform interior deposits, while Grammer et al. (1993b) showed that rapid lithification also occurs at the steep marginal slopes of Great Bahama Bank. Sea-level fluctuations will, therefore, automatically cause variations in the availability of certain grain types for export (as demonstrated for the Bahamas by Haak and Schlager, 1989) and the amount of certain grain sizes within the system (highstand shedding, Schlager et al., 1994; turbidite bundling, Droxler and Schlager, 1985, and Reijmer et al., 1988). Therefore, the way in which the different grain sizes are precisely distributed along the platform-to-basin transect from Site 1005 to Site 1006 during glacials and interglacials, forms the topic of ongoing research.

In addition, the composition of the coarse grains (>63 µm) exported from the platform during glacials and interglacials form the topic of further work in progress. However, first results confirm to a large extent the compositional variations within slope deposits of the Great Bahama Bank presented by Westphal et al. (1999) and within turbidites deposited in the Tongue of the Ocean (Haak and Schlager, 1989). The interglacial sediments are dominated by planktonic and benthic foraminifers and pteropods. The foraminifers present include *Globigerinina, Miliolina,* and, to a lesser extent, *Textulariina, Lagenina,* and *Rotaliina,* while the pteropods represented lie within the suborder *Eutheocosomata.* Also present are minor amounts of Echinoderm and Bryozoan fragments and some cortoids. In contrast, the glacial sediments are characterized by cortoids, whereby the bioclasts, peloids, and other particles are coated with a relatively thin micrite envelope. The cortoid grains consist typically of peloids, various planktonic foraminifers such as *Globigerinina* and *Miliolina,* and subangular quartz grains. These preliminary findings in compositional variations seen in interglacial and glacial sediments form the basis for a more detailed analysis, which is still in progress.

Kroon et al. (Chap. 2, this volume) observed a distinct difference in the isotope stratigraphy for the upper (>isotope Stage 11) and lower (= isotope Stage 11) part of Site 1006 and attributed these changes to increased sea-surface temperatures. The carbonate mineralogy and the grain-size distribution also seem to register this paleoceanographic change. The aragonite values show reduced values for Stages 9 and 11. In the upper-core section, the HMC percentages show a marked increase while the LMC percentages show a decrease. The grain-size distribution shows a sharp increase in the input of coarse (>63 µm) sediment since Stage 11. However, a more detailed analysis is needed to clarify the origin of these changes in greater detail.

CONCLUSIONS

Variations in the mineralogy and grain size of the sediment on the leeward side of the Great Bahama Bank have proved to be valuable in determining the platform response to climate changes. Trends characteristic of different environmental regimes through both time and space have become evident:

1. At the distal site (Hole 1006A), the $\delta^{18}O$ record and the aragonite record are well preserved and are in good agreement with each other. The proximal site, Hole 1003A, shows gaps in the sedimentary record, implying an erosional depositional regime on the platform slope. The $\delta^{18}O$ record here is also distorted because of diagenetic overprinting.
2. The interglacials (sea-level highstands) are dominated by the fine fraction (<63 µm), which shows no spacial variation in concentration. These sediments are predominantly neritic, bank-top derived aragonite needles exported off the platform. The carbonate mineralogy is dominated by aragonite, which decreases in concentration with increasing distance from the platform top. Within the subordinate coarse fraction (>63 µm), the very fine to medium sand-size fractions dominate. Dolomite appears as a product of early diagenesis at the proximal site. The terrigenous input (quartz) is very low. With increasing distance from the platform top, HMC and dolomite decrease in concentration, whereas LMC and quartz increase. These interglacial sediments have a low diagenetic potential because of low permeability and restricted fluid flow.
3. The glacials (sea-level lowstands) are clearly coarser grained but show a general decrease in coarse-sediment abundance with increasing distance from the platform top. The carbonate mineralogy for the fine fraction indicates that a mix of finer LMC-rich sediment was derived from pelagic input, and coarser HMC-rich sediment dominates these sediments. The HMC-rich sediment is derived from HMC-rich cements formed during early diagenesis and magnesium-calcite micrite cements from eroded upper slope material. Thus, with increasing distance from the platform, the LMC concentrations increase and the HMC concentrations decrease. Within the coarse fraction, the coarse to very coarse sand-size fractions dominate. Aragonite is in low concentrations because of relatively little neritic carbonate production and decreases in concentration with increasing distance from the platform top. Dolomite occurs in slightly higher concentrations, as does quartz. The dolomite shows the reverse spacial variation as seen during the interglacials, appearing in highest concentrations with quartz at the distal site, thus suggesting that glacial dolomite is of detrital origin. These glacial sediments have a high diagenetic potential because of high initial fluid flow and high permeability.
4. Because diagenesis has been shown to occur preferentially within coarse-grained sediments, it shows discontinuities both vertically and laterally within the sediment column because it is also dependent on the grain size of the sediment. Thus, it occurs on a vertical scale preferentially during glacials. As the grain size of the sediment decreases with increasing distance from the platform top, the diagenetic potential also decreases.
5. Grain size and mineralogy do not adequately describe coarse-grained, periplatform sediments. It is important to know the composition of the grains and whether they are pelagic or bank derived, skeletal or nonskeletal. Glacial sediments are characterized by cortoids, whereas planktonic and benthic foraminifers and pteropods dominate interglacial sediments. Further research is needed to see how these different types of grains are related to the observed grain size and mineralogical data.
6. Kroon et al. (Chap. 2, this volume) observed a period of possible surface-water warming during the Late Pleistocene at Site 1006 recorded in planktonic foraminifers. In our study, a distinct change in the mineralogy and grain size of the sediments was also observed at the same level. Since isotope Stage 11, the input of aragonite and HMC increases, whereas LMC decreases. The grain-size distribution shows that coarser sedi-

ments are deposited. Paleoceanographic changes might have been the cause for this shift in the overall sedimentation pattern on the Great Bahama Bank during this period.

ACKNOWLEDGMENTS

We thank the shipboard party and the Co-chiefs Gregor Eberli and Peter Swart of Leg 166 for collecting the samples and the staff of the ODP Core Repository in Bremen, Germany, for their assistance and hospitality during our stay to carry out additional subsampling. Also, we are very grateful to the research assistants, Steffen Zamhöfer and Marion Kötter, and our ODP Finnish representative Johanna Suhonen who conducted a great deal of the laboratory work. Thanks are also due to Christian Bühring for editorial help. We are grateful to GEOMAR in Germany and the Geology Department of Edinburgh University in Scotland for providing the facilities. We would especially like to thank Ian Alexander for his assistance in conducting the isotope measurements and Geoff Angell for his technical assistance during the XRD analysis. We are also grateful to R. Petschik for the MacDiff program, which aided in processing the XRD data. André Droxler and Geoff Haddad are thanked for their constructive reviews. Due thanks are also given to the German Science Foundation (DFG Re 1051/4), which provided the financial support.

REFERENCES

Berner, R.A., Berner, E.K., and Keir, R.S., 1976. Aragonite dissolution on the Bermuda Pedestal: its depth and geochemical significances. *Earth Planet. Sci. Lett.,* 30:169–178.

Betzler, C., Brachert, T.C., and Kroon, D., 1995. Role of climate in partial drowning of the Queensland plateau carbonate platform (northeastern Australia). *Mar. Geol.,* 123:11–32.

Boardman, M.R., and Neumann, A.C., 1984. Sources of periplatform carbonates: Northwest Providence Channel, Bahamas. *J. Sediment. Petrol.,* 54:1110–1112.

————, 1986. Reply on "Banktop responses to Quaternary fluctuations in sealevel recorded in periplatform sediments." *Geology,* 14:1040–1041.

Boardman, M.R., Neumann, A.C., Baker, P.A., Dulin, L.A., Kenter, R.J., Hunter, G.E., and Kiefer, K.B., 1986. Banktop responses to Quaternary fluctuations in sea level recorded in periplatform sediments. *Geology,* 14:28–31.

Boggs, S., Jr., 1987. Sedimentary textures. *In* Boggs, S., Jr. (Ed.), *Principles of Sedimentology and Stratigraphy:* New York (Macmillan), 105–122.

deMol, B., Westphal, H., and Reijmer, J.J.G., 1998. Correlation between geophysical and sedimentological properties in ODP Leg 166 Site 1005A. *15th Int. Sedimentol. Congr.,* 290–291. (Abstracts)

Dravis, J.J., 1996. Rapidity of freshwater calcite cementation: implications for carbonate diagenesis and sequence stratigraphy. *Sediment. Geol.,* 107:1–10.

Droxler, A.W., 1984. Late Quaternary glacial cycles in the Bahamian Deep Basins and in the adjacent ocean [Ph.D. dissert.]. Univ. Miami, Coral Gables, FL.

————, 1985. Last deglaciation in the Bahamas: a dissolution record from variations of aragonite content? *In* Sundquist, E.T., and Broecker, W.S. (Eds.), *The Carbon Cycle and Atmospheric CO_2: Natural Variations Archean to Present.* Geophys. Monogr., Am. Geophys. Union, 32:195–207.

————, 1986. Comment on "Banktop response to Quaternary fluctuations in sea level recorded in periplatform sediments." *Geology,* 14:1039–1040.

Droxler, A.W., Bruce, C.H., Sager, W.W., and Watkins, D.H., 1988. Pliocene-Pleistocene variations in aragonite content and planktonic oxygen-isotope record in Bahamian periplatform ooze, Hole 633A. *In* Austin, J.A., Jr., Schlager, W., et al., *Proc. ODP, Sci. Results,* 101: College Station, TX (Ocean Drilling Program), 221–244.

Droxler, A.W., Morse, J.W., Glaser, K.S., Haddad, G.A., and Baker, P.A., 1991. Surface sediment carbonate mineralogy and water column chemistry: Nicaragua Rise versus the Bahamas. *Mar. Geol.,* 100:277–289.

Droxler, A.W., and Schlager, W., 1985. Glacial versus interglacial sedimentation rates and turbidite frequency in the Bahamas. *Geology,* 13:799–802.

Droxler, A.W., Schlager, W., and Whallon, C.C., 1983. Quaternary aragonite cycles and oxygen-isotope record in Bahamian carbonate ooze. *Geology,* 11:235–239.

Dunham, R.J., 1962. Classification of carbonate rocks according to depositional texture. *In* Ham, W.E. (Ed.), *Classification of Carbonate Rocks.* AAPG Mem., 108–121.

Eberli, G.P., and Ginsburg, R.N., 1987. Segmentation and coalescence of Cenozoic carbonate platforms, northwestern Great Bahama Bank. *Geology,* 15:75–79.

————, 1989. Cenozoic progradation of the north western Great Bahamas Bank: a record of lateral platform growth and sea level fluctuations. *In* Crevello, P.D., Wilson, J.L., Sarg, J.F., and Read, J.F. (Eds.), *Controls on Carbonate Platform and Basin Development.* Spec. Publ.—Soc. Econ. Paleontol. Mineral., 44:339–351.

Eberli, G.P., Kendall, C.G., Moore, P., Whittle, G.L., and Cannon, R., 1994. Testing a seismic interpretation of Great Bahama Bank with a computer simulation. *AAPG Bull.,* 78:981–1004.

Eberli, G.P., Swart, P.K., Malone, M.J., et al., 1997. *Proc. ODP, Init. Repts.,* 166: College Station, TX (Ocean Drilling Program).

Eberli, G.P., Swart, P.K., McNeill, D.F., Kenter, J.A.M., Anselmetti, F.S., Melim, L.A., and Ginsburg, R.N., 1997. A synopsis of the Bahama Drilling Project: results from two deep sea core borings drilled on the Great Bahama Bank. *In* Eberli, G.P., Swart, P.K., Malone, M.J., et al., *Proc. ODP, Init. Repts.,* 166: College Station, TX (Ocean Drilling Program), 23–41.

Emery, D., 1996. Carbonate systems. *In* Emery, D., and Myers, K.J. (Eds.), *Sequence Stratigraphy:* Cambridge, England (Cambridge Univ. Press), 211–237.

Emery, D., and Myers, K.J., 1996. *Sequence Stratigraphy:* Cambridge, England (Cambridge Univ. Press).

Emiliani, C., 1978. The cause of the ice ages. *Earth Planet. Sci. Lett.,* 37:349–352.

Enos, P., 1974. Map of surface sediment facies of the Florida-Bahamas Plateau. *Geol. Soc. Am., Map Ser. MC-5,* no. 4.

Ginsburg, R.N., and James, N.P., 1976. Submarine botryoidal aragonite in Holocene reef limestones, Belize. *Geology,* 4:431–436.

Gischler, E., 1995. Current and wind induced facies patterns in a Devonian atoll: Iberg Reef, Harz Mts., Germany. *Palaios,* 10:180–189.

Glaser, K.S., and Droxler, A.W., 1993. Controls and development of late Quaternary periplatform carbonate stratigraphy in Walton Basin (northeastern Nicaragua Rise, Caribbean Sea). *Paleoceanography,* 8: 243–274.

Grammer, G.M., and Ginsburg, R.N., 1992. Highstand versus lowstand deposition on carbonate platform margins: insight from Quaternary foreslopes in the Bahamas. *Mar. Geol.,* 103:125–136.

Grammer, G.M., Ginsburg, R.N., and Harris, P.M., 1993. Timing of deposition, diagenesis, and failure of steep carbonate slopes in response to a high-amplitude/high-frequency fluctuation in sea level, Tongue of the Ocean, Bahamas. *In* Loucks, R.G., and Sarg, J.F. (Eds.), *Carbonate Sequence Stratigraphy: Recent Developments and Applications.* AAPG Mem., 57:107–131.

Grammer, G.M., Ginsburg, R.N., and McNeill, D.F., 1991. Morphology and development of modern carbonate foreslopes, Tongue of the Ocean, Bahamas. *In* Larue, D.K., and Draper, G. (Eds.), *Trans. 12th Caribbean Geol. Conf.,* 27–32.

Grammer, G.M., Ginsburg, R.N., Swart, P.K., McNeill, D.F., Jull, A.T., and Prezbindowski, D.R., 1993. Rapid growth rates of syndepositional marine aragonite cements in steep marginal slope deposits, Bahamas and Belize. *J. Sediment. Petrol.,* 63:983–989.

Haak, A.B., and Schlager, W., 1989. Compositional variations in calciturbidites due to sea-level fluctuations, Late Quaternary, Bahamas. *Geol. Rundsch.,* 78:477–486.

Haddad, G.A., and Droxler, A.W., 1996. Metastable $CaCO_3$ dissolution at intermediate water depths of the Caribbean and western North Atlantic: implications for intermediate water circulation during the past 200,000 years. *Paleoceanography,* 11:701–716.

Handford, C.R., and Loucks, R.G., 1993. Carbonate depositional sequences and systems tracts: responses of carbonate platforms to relative sea-level changes. *In* Loucks, R.G., and Sarg, J.F. (Eds.), *Carbonate Sequence Stratigraphy.* AAPG Mem., 57:3–41.

Hine, A.C., Wilber, R.J., Bane, J.M., Neumann, A.C., and Lorenson, K.R., 1981. Offbank transport of carbonate sands along open, leeward bank margins: northern Bahamas. *Mar. Geol.,* 42:327–348.

Hine, A.C., Wilber, R.J., and Neumann, C., 1981. Carbonate sand bodies along contrasting shallow bank margins facing open seaways in northern Bahamas. *AAPG Bull.,* 65:261–290.

Johnson, J.H., 1961. *Limestone-building Algae and Algal Limestones:* Boulder (Colorado School of Mines).

Kendall, C.G.St.C., and Schlager, W., 1981. Carbonates and relative changes in sea level. *In* Cita, M.B., and Ryan, W.B.F. (Eds.), *Carbonate Platforms*

of the Passive-type Continental Margins, Present and Past. Mar. Geol., 44:181–212.

Kenter, J.A.M., 1990. Carbonate platform flanks: slope angle and sediment fabric. *Sedimentology,* 37:777–794.

Kindler, P., and Hearty, P.J., 1996. Carbonate petrography as an indicator of climate and sea-level changes: new data from Bahamian Quaternary units. *Sedimentology,* 43:381–399.

Lynts, G.W., Judd, J.B., and Stehman, C.F., 1973. Late Pleistocene history of Tongue of the Ocean, Bahama. *Geol. Soc. Am. Bull.,* 84:2605–2684.

Macintyre, I.G., and Reid, R.P., 1992. Comment on the origin of aragonite needle mud: a picture is worth a thousand words. *J. Sediment. Petrol.,* 62:1095–1097.

Milliman, J.D., 1974. Carbonates and the ocean. *In* Milliman, J.D. (Ed.), *Marine Carbonates* (Pt 1): New York (Springer-Press), 3–15.

Milliman, J.D., Freile, D., Steinen, R., and Wilber, R.J., 1993. Great Bahama Bank aragonitic muds: mostly inorganically precipitated, mostly exported. *J. Sediment. Petrol.,* 63:589–595.

Mullins, H.T., 1983. Comment on "Eustatic control of turbidites and winnowed turbidites." *Geology,* 11:57–58.

Mullins, H.T., Neumann, A.C., Wilber, R.J., Hine, A.C., and Chinsburg, S.J., 1980. Carbonate sediment drifts in the northern Straits of Florida. *AAPG Bull.,* 64:1701–1717.

Mullins, H.T., Wise, S.W., Jr., Land, L.S., Siegel, D.I., Masters. P.M., Hinchey, E.J., and Price, K.R., 1985. Authigenic dolomite in Bahamian periplatform slope sediment. *Geology,* 13:292–295.

Neumann, A.C., and Land, L.S., 1975. Lime mud deposition and calcareous algae in the Bight of Abaco, Bahamas: a budget. *J. Sediment. Petrol.,* 45:763–786.

Pilkey, O.H., and Rucker, J.B., 1966. Mineralogy of Tongue of the Ocean sediments. *J. Mar. Res.,* 24:276–285.

Purdy, E.G., 1963. Recent calcium carbonate facies of the Great Bahama Bank, 2: Sedimentary facies. *J. Geol.,* 71:472–497.

Reijmer, J.J.G., Schlager, W., and Droxler, A.W., 1988. ODP Site 632: Pliocene-Pleistocene sedimentation cycles in a Bahamian basin. *In* Austin, J.A., Jr., Schlager, W., et al., *Proc. ODP, Sci. Results,* 101: College Station, TX (Ocean Drilling Program), 213–220.

Robbins, L.L., Tao, Y., and Evans, C.A., 1997. Temporal and spatial distribution of whitings on Great Bahama Bank and a new lime mud budget. *Geology,* 25:947–950.

Schlager, W., and Camber, O., 1986. Submarine slope angles, drowning unconformities, and self-erosion of limestone escarpments. *Geology,* 14:762–765.

Schlager, W., and James, N.P., 1978. Low-magnesian calcite limestones forming at the deep-sea floor, Tongue of the Ocean, Bahamas. *Sedimentology,* 25:675–702.

Schlager, W., Reijmer, J., and Droxler, A.W., 1994. Highstand shedding of carbonate platforms, *J. Sediment. Res.,* B64:270–281.

Scholle, P.A., Arthur, M.A., and Ekdale, A.A., 1983. Pelagic environments. *In* Scholle, P.A., Bebout, D.G., and Moore, C.H. (Eds.), *Carbonate Depositional Environments.* AAPG Mem., 33:620–691.

Shackleton, N.J., and Opdyke, N.D., 1973. Oxygen isotope and paleomagnetic stratigraphy of equatorial Pacific core V28-238: oxygen isotope temperatures and ice volumes on a 10^5 year and 10^6 year scale. *Quat. Res.,* 3:39–55.

Slowey, N.C., Henderson, G.M., and Curry, W.B., 1996. Direct U-Th dating of marine sediments from the two most recent interglacial periods. *Nature,* 383:242–244.

Tucker, M.E., 1985. Shallow marine carbonate facies and facies models. *In* Brenchley, P.J., and Williams, B.P.J. (Eds.), *Sedimentology: Recent Development and Applied Aspects.* Geol. Soc. Spec. Publ. London, 18:139–161.

Tucker, M.E., and Wright, P.V., 1990. *Carbonate Sedimentology:* Oxford (Blackwell Sci. Publ.).

Wentworth, C.K., 1922. A scale of grade and class terms of clastic sediments. *J. Geol.,* 30:377–392.

Westphal, H., 1997. Sediment input and diagenesis of periplatform carbonates on a leeward slope of Great Bahama Bank [Ph.D. thesis]. Christian-Albrechts-Univ. zu Kiel, Germany.

Westphal, H., Reijmer, J.J.G., and Head, M.J., 1999. Sedimentary input and diagenesis on a carbonate slope (Bahamas): response to morphology evolution of the platform and sea level fluctuations. *In* Harris, P.M., Saller, A.H., and Simo, T. (Eds.), *Advances in Carbonate Sequence Stratigraphy: Application to Reservoirs, Outcrops, and Models*. Spec. Publ.—Soc. Econ. Paleontol. Mineral., 63:247–274.

Wilber, R.J., Milliman, J.D., and Halley, R.B., 1990. Accumulation of bank-top sediment on the western slope of Great Bahama Bank: rapid progradation of a carbonate megabank. *Geology,* 18:970–974.

Wilson, P.A., and Roberts, H.H., 1995. Density cascading: off-shelf sediment transport, evidence and implications, Bahama Banks. *J. Sediment. Res.,* A65:45–56.

Wolf, T.C.W., and Thiede, J., 1991. History of terrigenous sedimentation during the past 10 m.y. in the North Atlantic (ODP Legs 104 and 105 and DSDP Leg 81). *Mar. Geol.,* 101:83–102.

Date of initial receipt: 19 August 1998
Date of acceptance: 28 August 1999
Ms 166SR-114